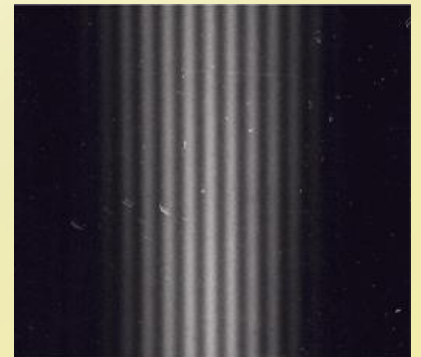
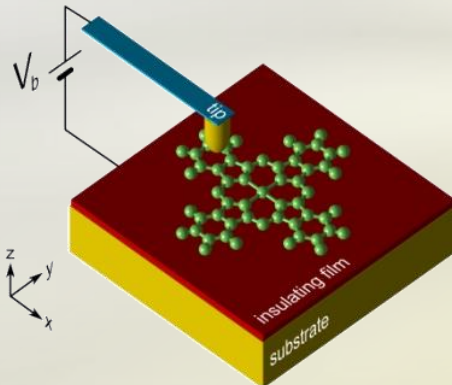


STM on thin insulating films: a density matrix approach

Andrea Donarini

Sandra Sobczyk, Benjamin Siegert and Milena Grifoni

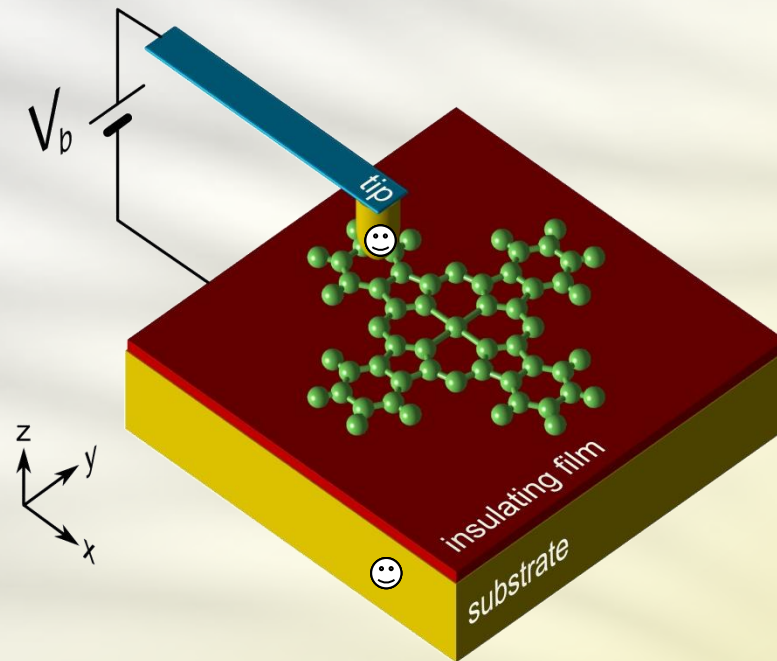
University of Regensburg, Germany



Outline

- **Scanning Tunnelling Microscopy** (STM) on thin insulating films
- **Interference** in electron transport measurements
- **Density matrix** approach to STM
- **Interference effects** in transport through **Cu-Phthalocyanine**
- **Conclusions** and **outlook**

STM on thin insulating films



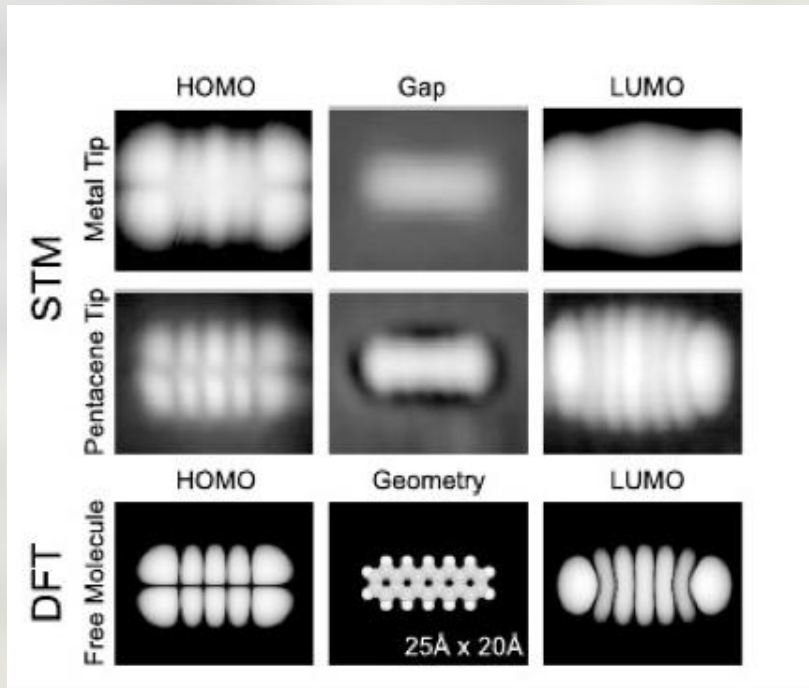
Weak tip-molecule tunnelling coupling
Low molecule-substrate hybridization



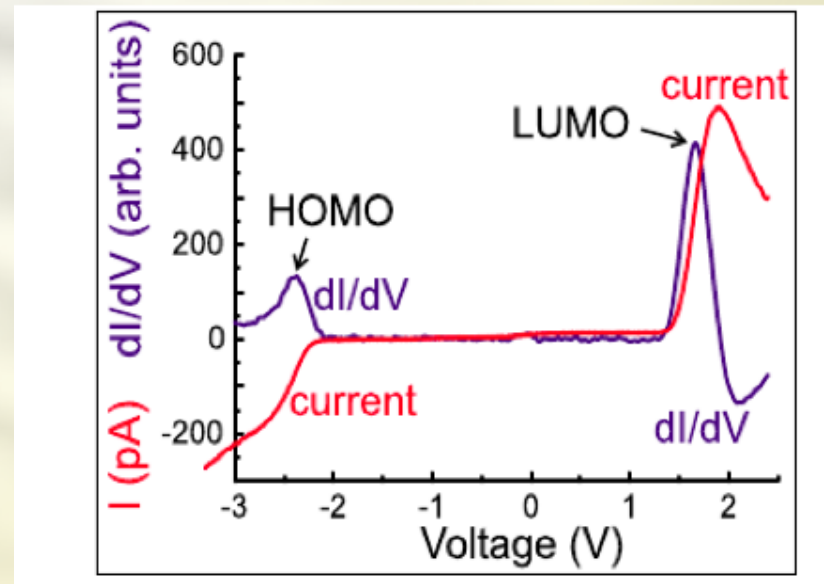
sequential tunnelling

Visualization of molecular orbitals

Topography

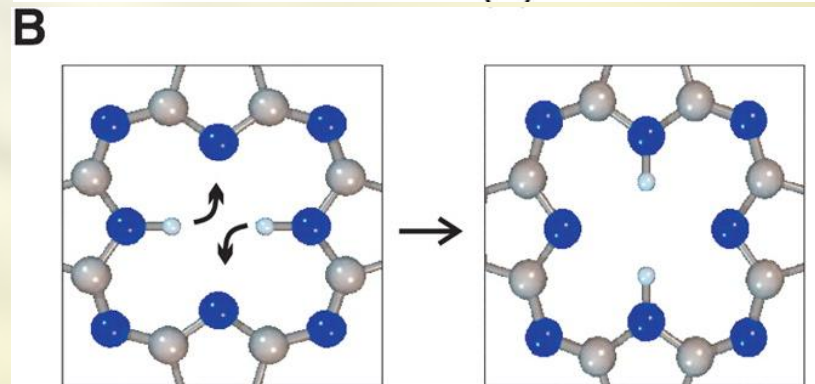
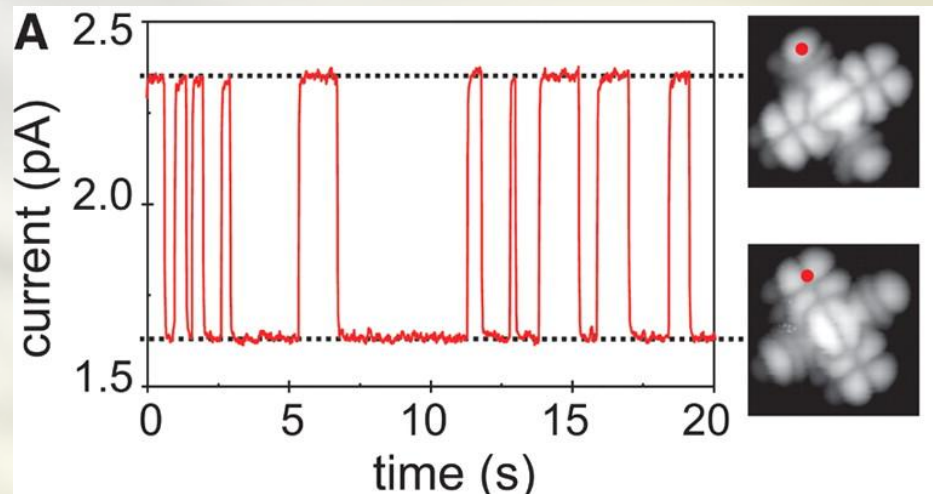
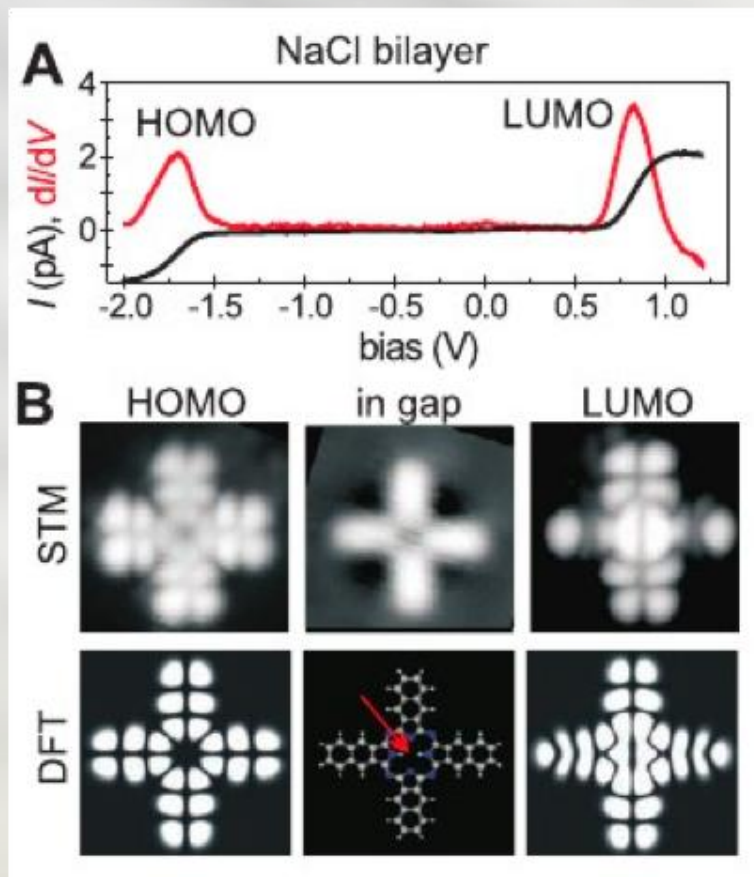


Spectroscopy



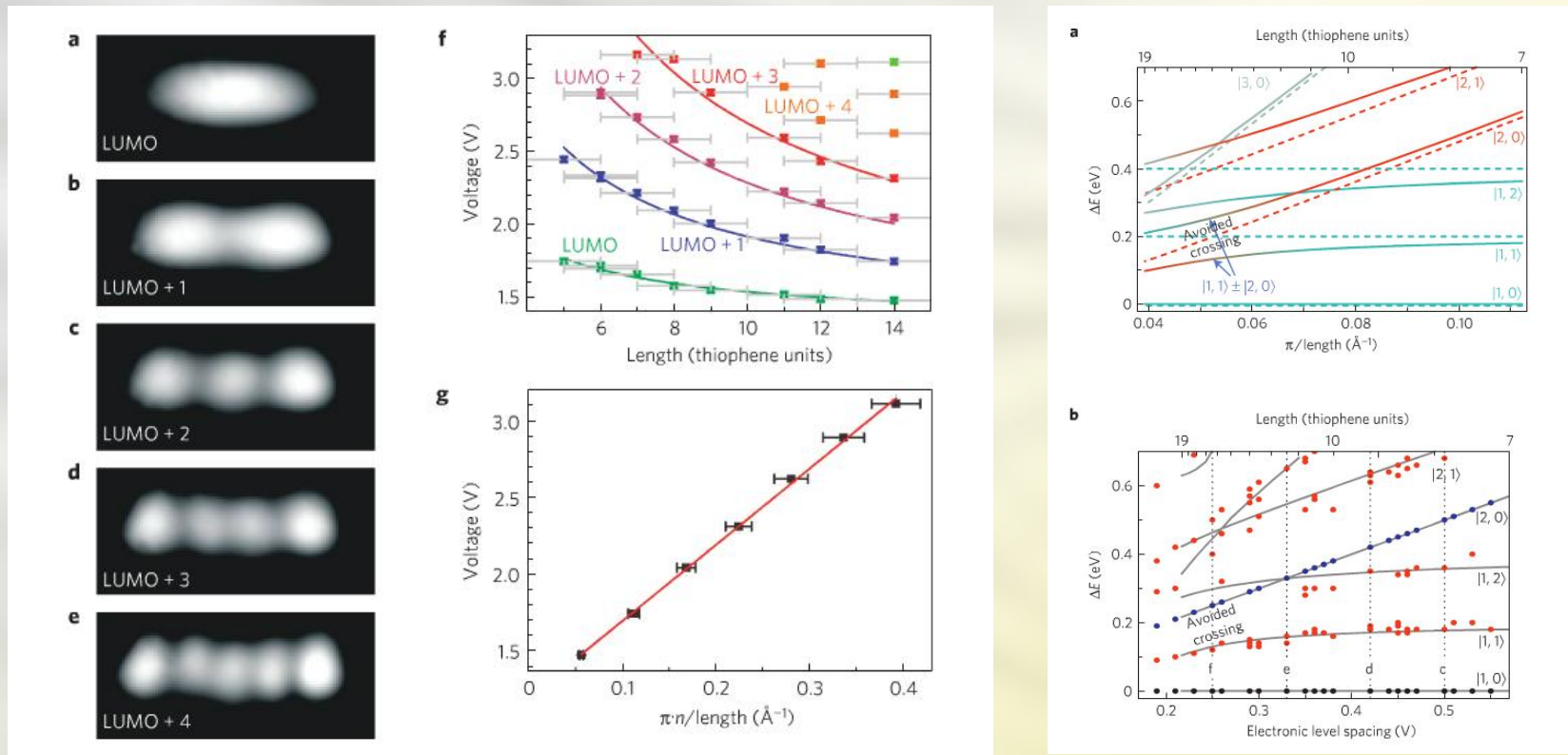
J. Repp and G. Meyer, Physical Review Letters **94**, 026803 (2005)

Tautomerization and switching



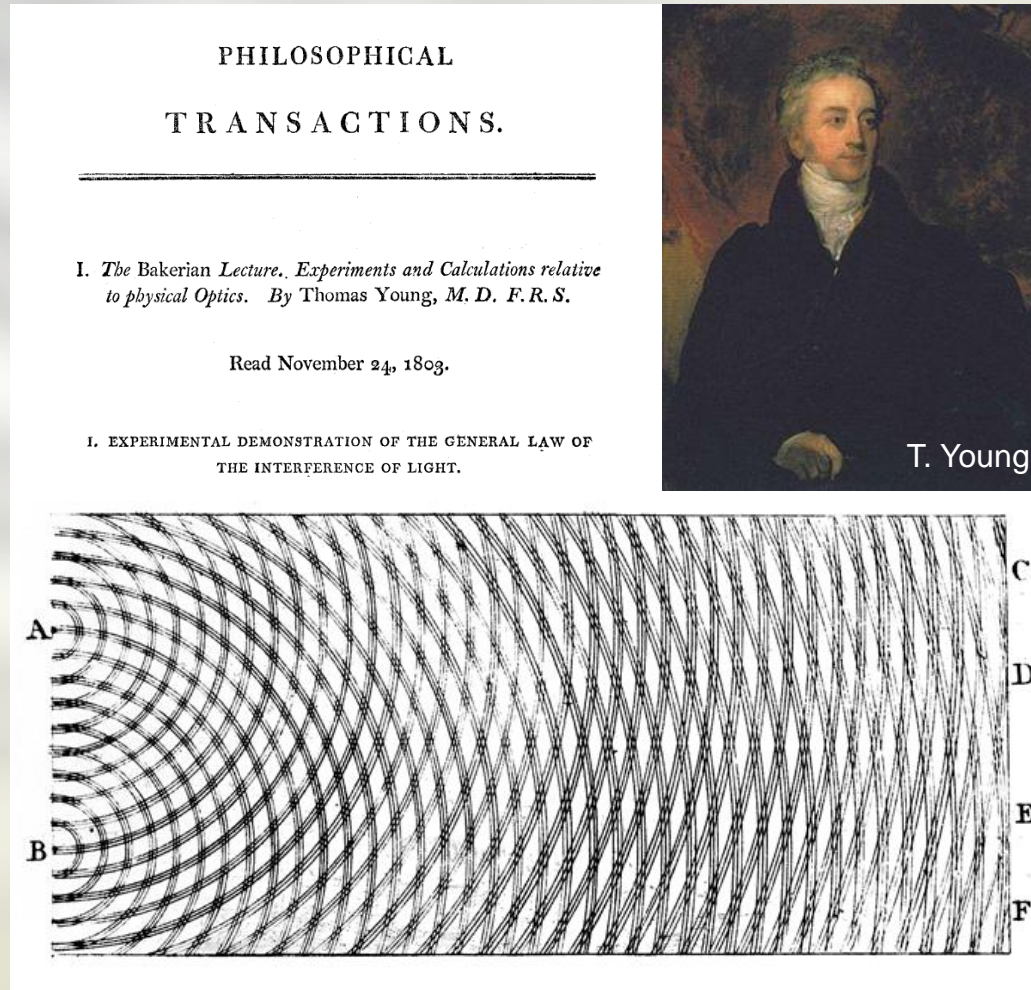
P. Liljeroth, J. Repp, G. Meyer, *Science* **317**, 1203 (2007)

Electro-mechanical entanglement



J. Repp, P. Liljeroth, G. Meyer, Nature Physics **6**, 975 (2010)

Double slit experiment: (London, 1801)



Phil. Trans. R. Soc. Lon., **94**, 12 (1804)

Double slit with electrons: (Tübingen, 1961)

Aus dem Institut für Angewandte Physik der Universität Tübingen

Elektroneninterferenzen an mehreren künstlich hergestellten Feinspalten

Von

CLAUS JÖNSSON

Mit 14 Figuren im Text

(Eingegangen am 17. Oktober 1960)

A glass plate covered with an evaporated silver film of about 200 Å thickness is irradiated by a line-shaped electron-probe in a vacuum of 10^{-4} Torr. A hydrocarbon polymerisation film of very low electrical conductivity is formed at places subjected to high electron current density. An electrolytically deposited copper film leaves these places free from copper. When the copper film is stripped a grating with slits free of any material is obtained. $50\ \mu$ long and $0.3\ \mu$ wide slits with a grating constant of $1\ \mu$ are obtained. The maximum number of slits is five. The electron diffraction pattern obtained using these slits in an arrangement analogous to Young's light optical interference experiment in the Fraunhofer plane and Fresnel region shows an effect corresponding to the well-known interference phenomena in light optics.

Zeitschrift für Physik, **161**, 454 (1961)



C.Jönsson



Single electron interference (Bologna, 1974)

On the statistical aspect of electron interference phenomena

P. G. Merli

CNR-LAMEL, Bologna, Italy

G. F. Missiroli and G. Pozzi

CNR-GNSM, Istituto di Fisica, Laboratorio Microscopia Elettronica, Bologna, Italy

(Received 29 May 1974; revised 17 October 1974)

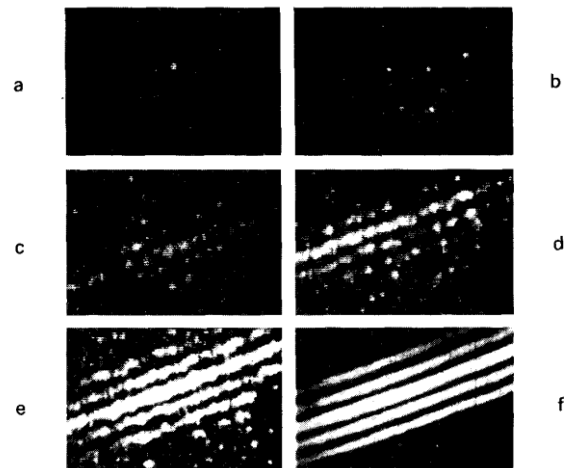


Fig. 1. (a-f) Electron interference fringe patterns filmed from a TV monitor at increasing current densities.

Am. J. Phys., **44**, 306 (1976)

Demonstration of single-electron buildup of an interference pattern

A. Tonomura, J. Endo, T. Matsuda, and T. Kawasaki
Advanced Research Laboratory, Hitachi, Ltd., Kokubunji, Tokyo 185, Japan

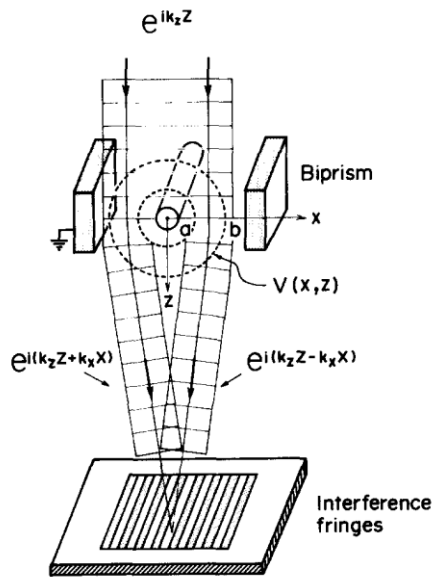
H. Ezawa
Department of Physics, Gakushuin University, Mejiro, Tokyo 171, Japan

(Received 17 December 1987; accepted for publication 22 March 1988)

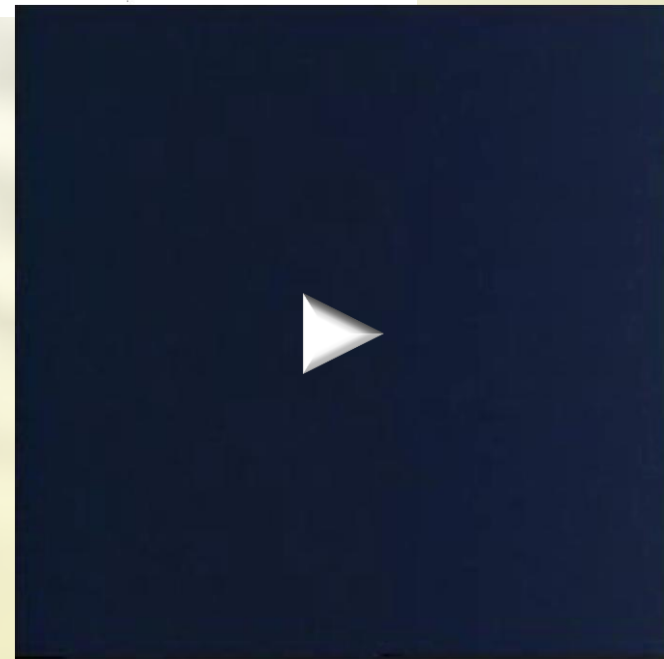
The wave-particle duality of electrons was demonstrated in a kind of two-slit interference experiment using an electron microscope equipped with an electron biprism and a position-sensitive electron-counting system. Such an experiment has been regarded as a pure thought experiment that can never be realized. This article reports an experiment that successfully recorded the actual buildup process of the interference pattern with a series of incoming single electrons in the form of a movie.



A. Tonomura



Am. J. Phys., **57**, 117 (1989)



Coherence and Phase Sensitive Measurements in a Quantum Dot

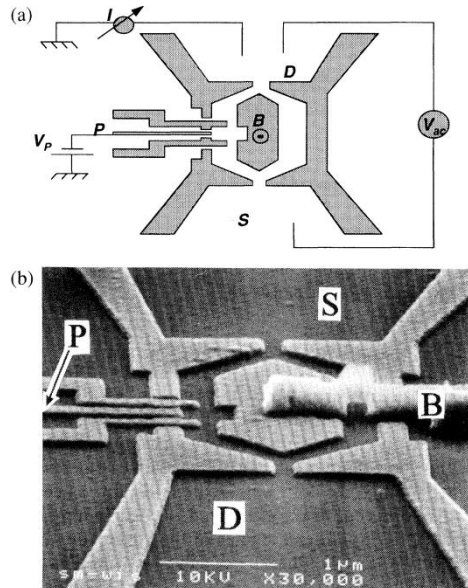
A. Yacoby, M. Heiblum, D. Mahalu, and Hadas Shtrikman

Braun Center for Submicron Research, Department of Condensed Matter Physics, Weizmann Institute of Science, Rehovot 76100, Israel

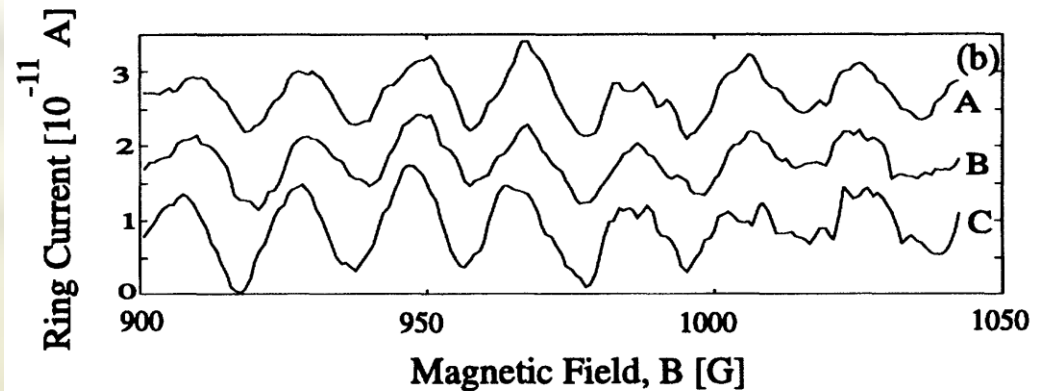
(Received 10 November 1994)

Via a novel interference experiment, which measures magnitude and *phase* of the transmission coefficient through a quantum dot in the Coulomb regime, we prove directly, for the first time, that transport through the dot has a coherent component. We find the same phase of the transmission coefficient at successive Coulomb peaks, each representing a different number of electrons in the dot; however, as we scan through a single Coulomb peak we find an *abrupt* phase change of π . The observed behavior of the phase cannot be understood in the single particle framework.

PACS numbers: 73.20.Dx, 71.45.-d, 72.80.Ey, 73.40.Gk



M. Heiblum

*Phys. Rev. Lett.*, **74**, 4047 (1995)

...counting single electrons (Zürich, 2008)

Time-Resolved Detection of Single-Electron Interference

S. Gustavsson,* R. Leturcq, M. Studer, T. Ihn, and K. Ensslin

Solid State Physics Laboratory, ETH Zürich, CH-8093 Zürich, Switzerland

D. C. Driscoll and A. C. Gossard

Materials Department, University of California, Santa Barbara, California 93106

Received June 13, 2008

NANO
LETTERS

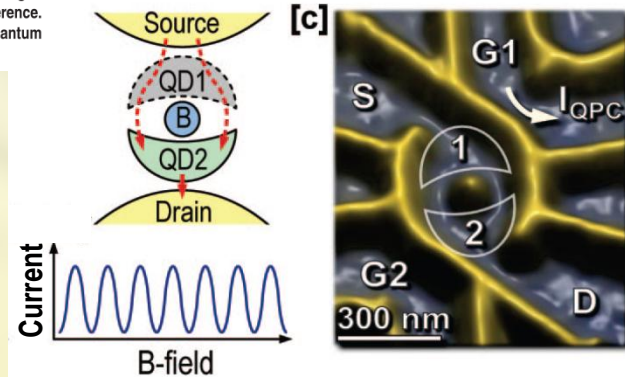
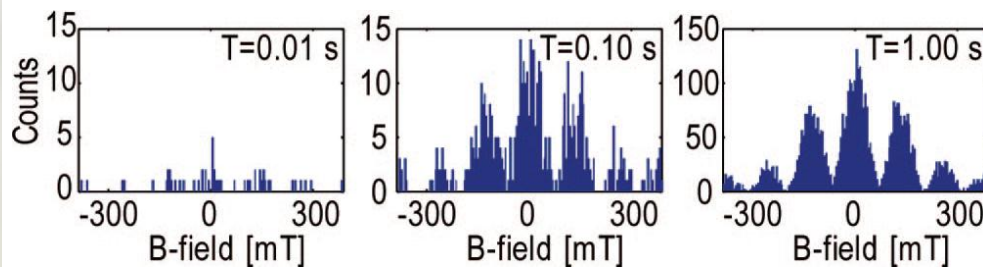
2008
Vol. 8, No. 8
2547-2550



K. Ensslin

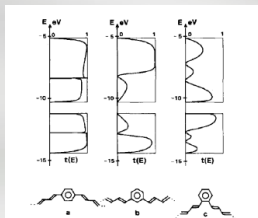
ABSTRACT

We demonstrate real-time detection of self-interfering electrons in a double quantum dot embedded in an Aharonov–Bohm interferometer, with visibility approaching unity. We use a quantum point contact as a charge detector to perform time-resolved measurements of single-electron tunneling. With increased bias voltage, the quantum point contact exerts a back-action on the interferometer leading to decoherence. We attribute this to emission of radiation from the quantum point contact, which drives noncoherent electronic transitions in the quantum dots.

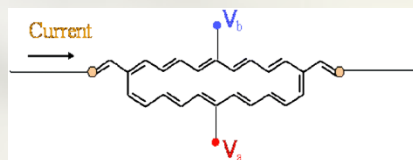


Nano Lett., **8**, 2547 (2008)

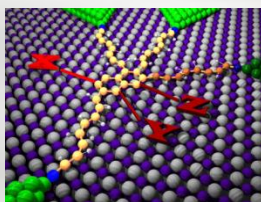
Intramolecular interference: theoretical proposals



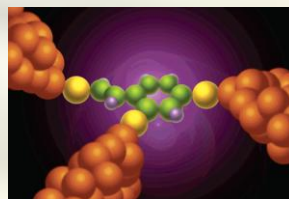
P. Sautet and C. Joachim
Chem. Phys. Lett. **153**, 511 (1988)



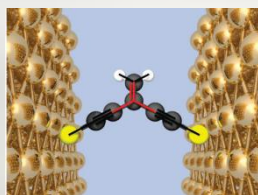
R. Baer and D. Neuhauser
JACS, **124**, 4200 (2002)



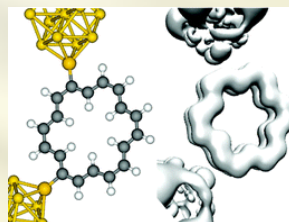
R. Stadler, et al.
Nanotechnology, **14**, 138 (2003)



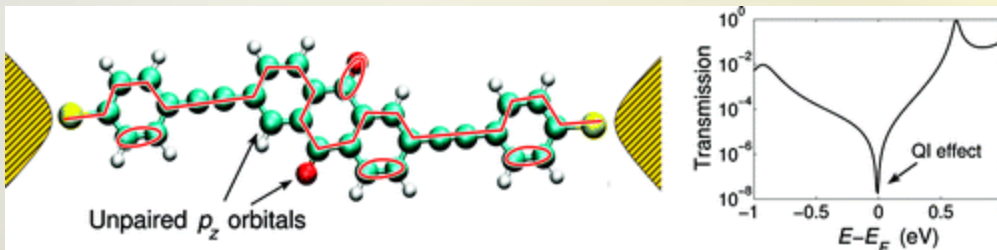
D. V. Cardamone, et al.
Nano Lett., **6**, 2422 (2006)



G. Solomon, et al.
JACS **130**, 17307 (2008)

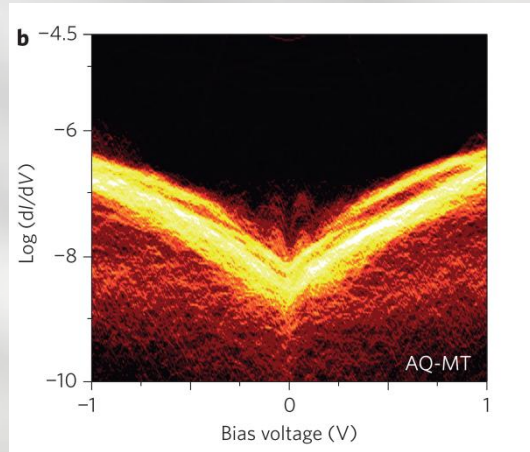


S.H. Ke, et al.
Nano Lett., **8**, 3257 (2008)

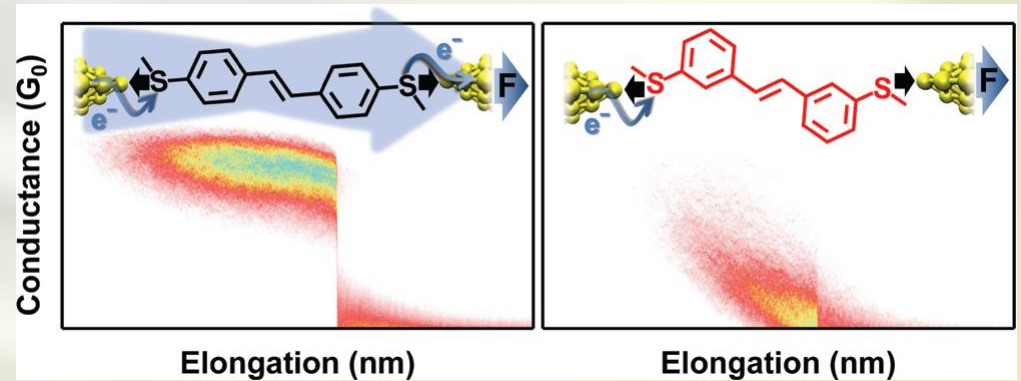


T. Markussen, et al.
Nano Lett., **10**, 4260 (2010)

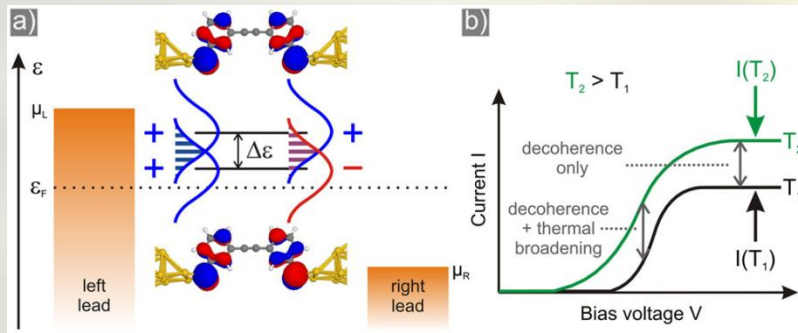
Experimental evidence



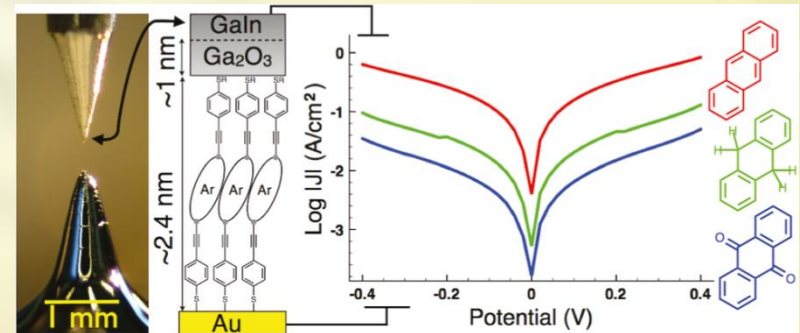
Guédon et al. *Nature Nanotech.* **7**, 305 (2012)



Aradhy et al. *Nano Lett.*, **12**, 1643 (2012)

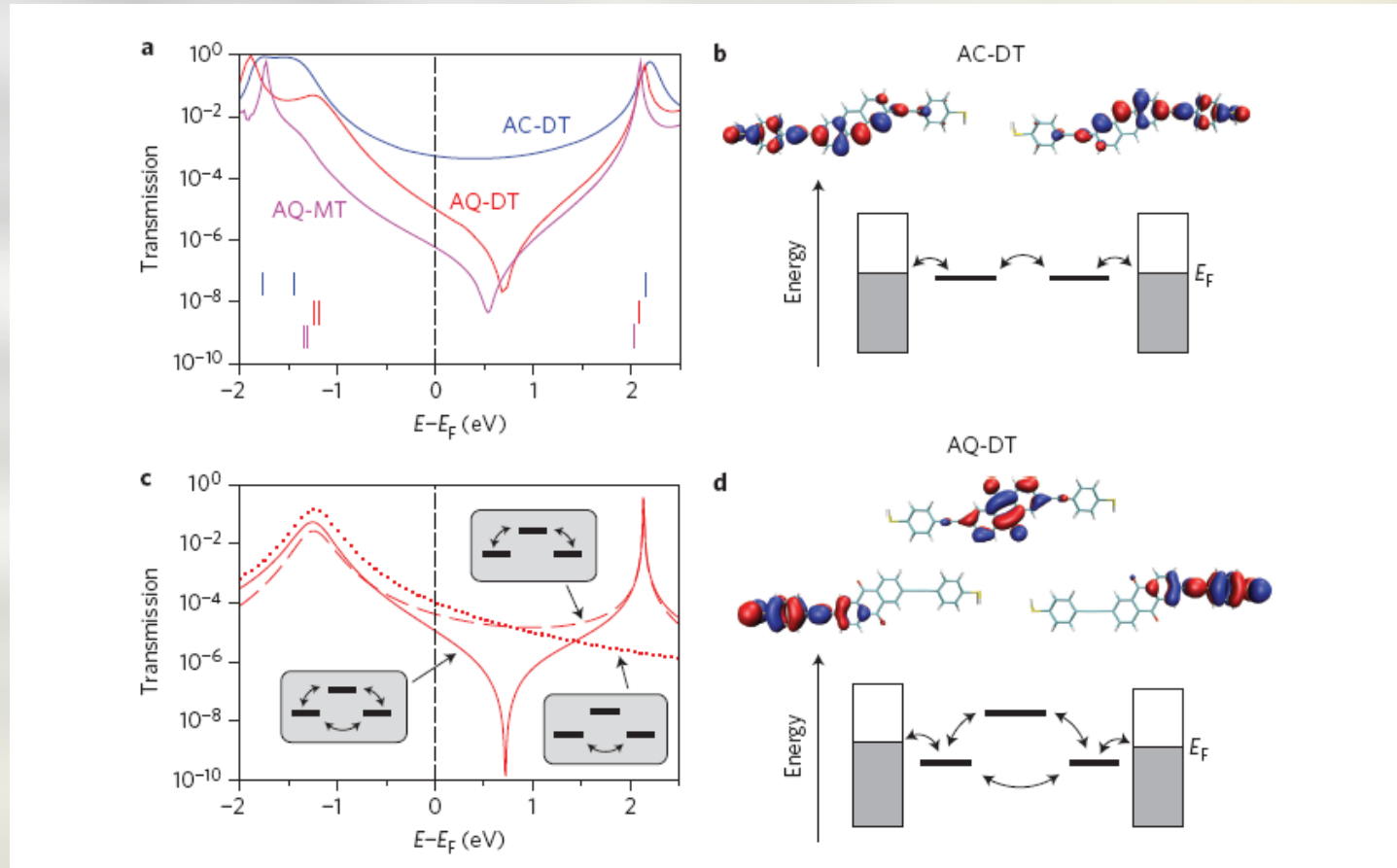


Ballman et al. *PRL* 109, 056801 (2012)



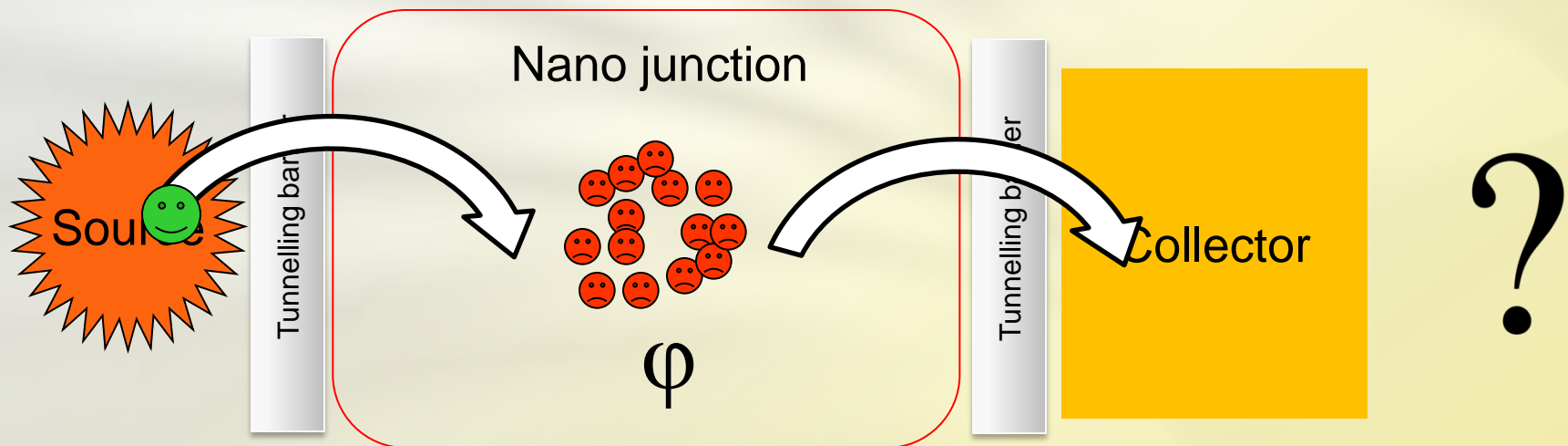
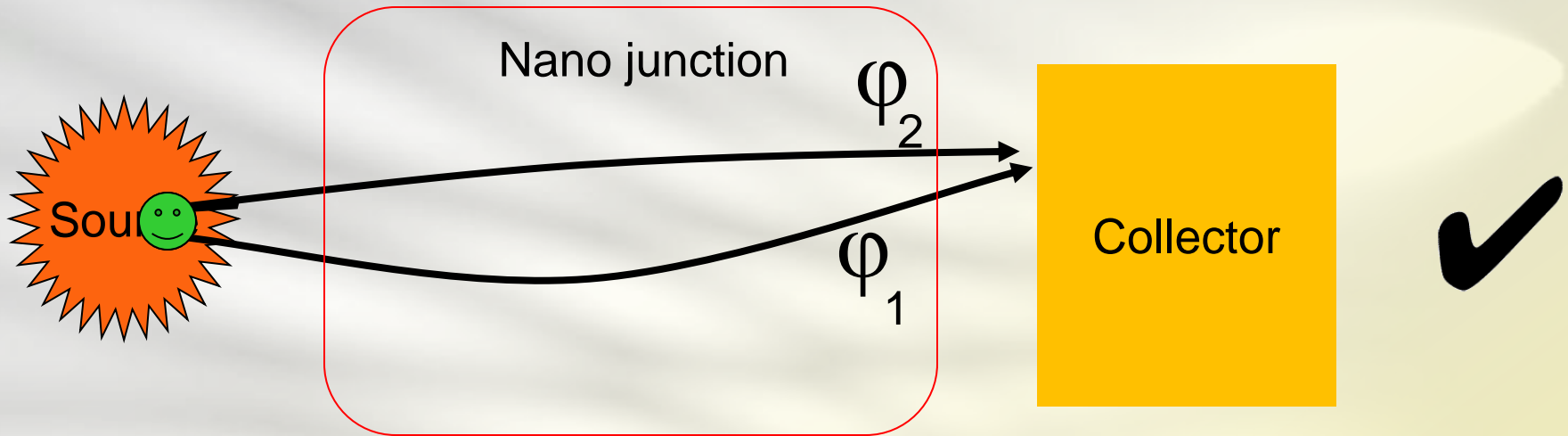
Fracasso et al. *JACS*, **133**, 9556 (2011)

Destructive interference



C. M. Guedon, H. Valkenier et al. *Nature Nanotech.* **7**, 305 (2012)

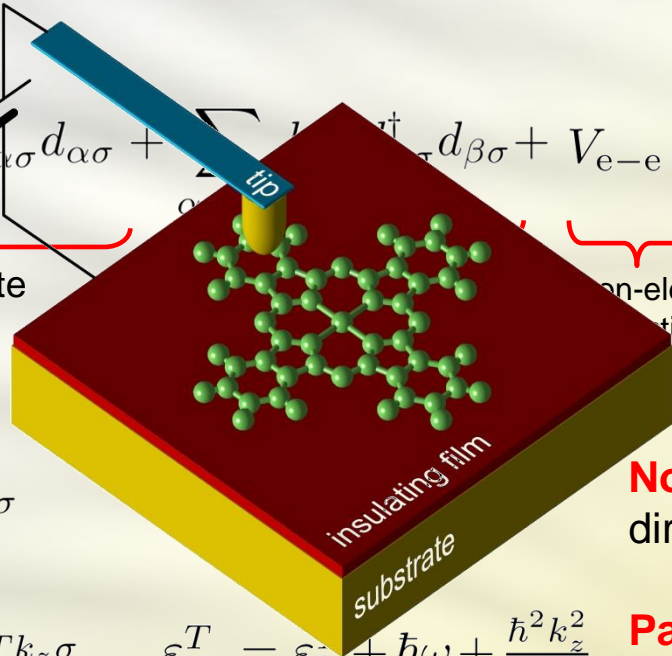
Interference and dephasing



Model of the STM junction

$$H = H_m + H_{\text{sub}} + H_{\text{tip}} + H_{\text{tun}}$$

$$H_m = \underbrace{\sum_{\alpha\sigma} v_{\alpha\alpha} d_{\alpha\sigma}^\dagger d_{\alpha\sigma}}_{\text{on-site}} + \underbrace{\sum_{\alpha\beta\sigma} t_{\alpha\beta} d_{\alpha\sigma}^\dagger d_{\beta\sigma} + V_{e-e}}_{\text{on-electron interaction}} \left\{ \begin{array}{l} \text{Hubbard} \\ \text{Extended Hubbard} \\ \text{Constant interaction} \end{array} \right.$$



$$H_{\text{sub}} = \sum_{\vec{k}\sigma} \varepsilon_{\vec{k}}^S c_{S\vec{k}\sigma}^\dagger c_{S\vec{k}\sigma}$$

No confinement in the x-y directions

$$H_{\text{tip}} = \sum_{k_z\sigma} \varepsilon_{k_z}^T c_{Tk_z\sigma}^\dagger c_{Tk_z\sigma} \quad \varepsilon_{k_z}^T = \varepsilon_0 + \hbar\omega + \frac{\hbar^2 k_z^2}{2m}$$

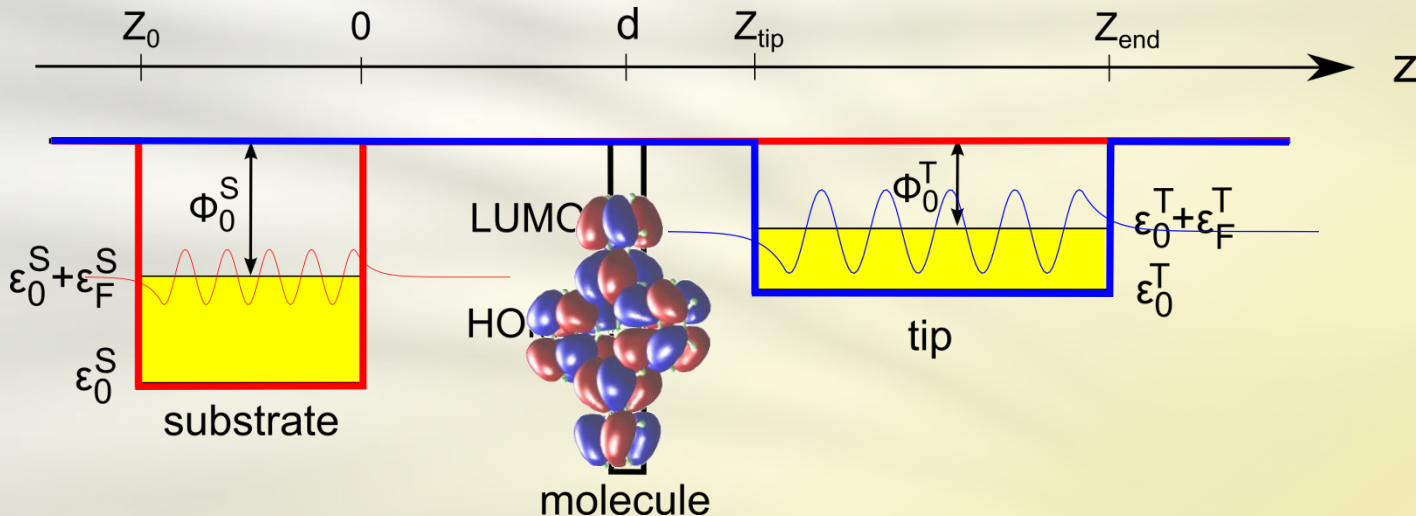
Parabolic confinement in the x-y directions

$$H_{\text{tun}} = \sum_{\chi k i \sigma} t_{ki}^\chi c_{\chi k \sigma}^\dagger d_{i\sigma} + h.c. \quad \text{It is a **single particle** operator}$$

← Molecular orbital

Tunnelling amplitudes

$$h = \frac{p^2}{2m} + v_m + v_{\text{sub}} + v_{\text{tip}} \quad t_{ki}^\chi := \langle \chi k \sigma | h | i \sigma \rangle$$



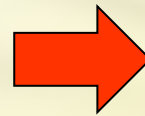
Tunnelling amplitudes (ii)

$$t_{ki}^{\chi} = \langle \chi k \sigma | \frac{p^2}{2m} + v_m | i \sigma \rangle + \langle \chi k \sigma | v_{\text{sub}} + v_{\text{tip}} | i \sigma \rangle$$

$$= \varepsilon_i \langle \chi k \sigma | i \sigma \rangle$$

Valence atomic orbitals
larger in the leads than
in the molecule

More perpendicular nodal planes
in the molecule than in the leads



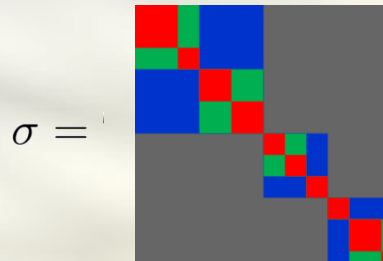
$$\psi_{\chi k}(\vec{r}) \phi_i(\vec{r})$$

is **shifted towards
the molecule**

Generalized Master Equation

- We start with the **Liouville** equation: $\dot{\rho} = -\frac{i}{\hbar}[H, \rho]$

- We define the reduced density matrix $\sigma = \text{Tr}_{S+T}\{\rho\}$ which is **block-diagonal** in

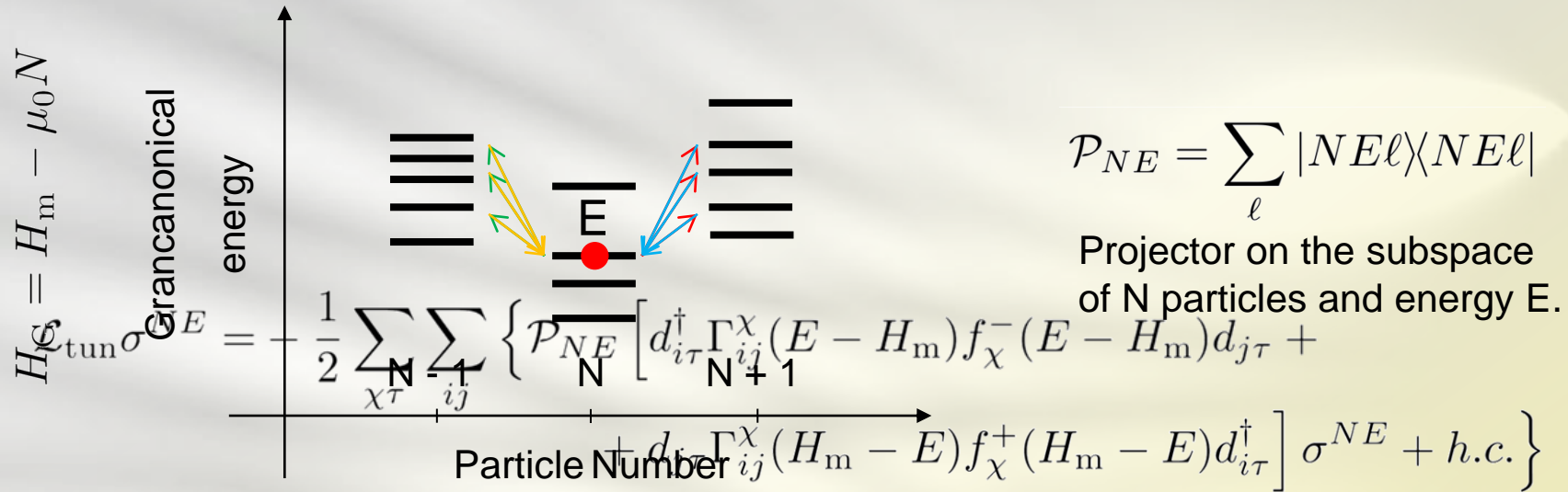


particle number
spin
energy

- We keep the coherences between **orbitally** degenerate states.
- The **Generalized Master Equation** is the equation of motion for σ :

$$\dot{\sigma} = \underbrace{-\frac{i}{\hbar}[H_m, \sigma]}_{\text{Coherent dynamics}} - \underbrace{\frac{i}{\hbar}[H_{\text{eff}}, \sigma]}_{\text{Effective internal dynamics}} + \underbrace{\mathcal{L}_{\text{tun}}\sigma}_{\text{Tunnelling dynamics}} := \mathcal{L}\sigma$$

Tunnelling Liouvillean



$$\mathcal{P}_{NE} = \sum_{\ell} |NE\ell\rangle\langle NE\ell|$$

Projector on the subspace of N particles and energy E.

$$+ \sum_{\chi\tau} \sum_{ijE'} \mathcal{P}_{NE} \left[d_{i\tau}^\dagger \Gamma_{ij}^\chi (E - E') \sigma^{N-1E'} f_\chi^+(E - E') d_{j\tau} + d_{j\tau} \Gamma_{ij}^\chi (E' - E) \sigma^{N+1E'} f_\chi^-(E' - E) d_{i\tau}^\dagger \right] \mathcal{P}_{NE}$$

Single particle rate matrix

$$\Gamma_{ij}^{\chi}(\Delta E) = \frac{2\pi}{\hbar} \sum_k (t_{ki}^{\chi})^* t_{kj}^{\chi} \delta(\varepsilon_k^{\chi} - \Delta E)$$

$$H_{\text{eff}} = \frac{1}{2\pi} \sum_{NE} \sum_{\chi\sigma} \sum_{ij} \mathcal{P}_{NE} \left[d_{i\sigma}^{\dagger} \Gamma_{ij}^{\chi}(E - H_m) p_{\chi}(E - H_m) d_{j\sigma} \right. \\ \left. + d_{j\sigma} \Gamma_{ij}^{\chi}(H_m - E) p_{\chi}(H_m - E) d_{i\sigma}^{\dagger} \right] \mathcal{P}_{NE}$$

Effective
Hamiltonian

$$I_{\chi} = \sum_{NE\sigma ij} \mathcal{P}_{NE} \left[d_{j\sigma} \Gamma_{ij}^{\chi}(H_m - E) f_{\chi}^{+}(H_m - E) d_{i\sigma}^{\dagger} \right. \\ \left. - d_{i\sigma}^{\dagger} \Gamma_{ij}^{\chi}(E - H_m) f_{\chi}^{-}(E - H_m) d_{j\sigma} \right] \mathcal{P}_{NE}$$

Current
operator

Many-body rate matrix

The **current** is proportional to the **transition rate** between **many-body states**

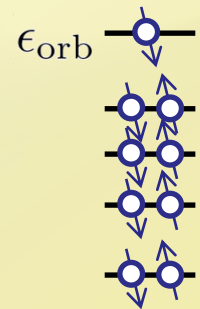
$$R_{N E_0 \rightarrow N+1 E_1}^{\chi\tau} = \sum_{ij} \langle N+1 E_1 | d_{i\tau}^\dagger | N E_0 \rangle \Gamma_{ij}^\chi(E_1 - E_0) \times \\ \langle N E_0 | d_{j\tau} | N+1 E_1 \rangle f^+(E_1 - E_0 - \mu_\chi)$$

where

$$\Gamma_{ij}^\chi(E_1 - E_0) = \frac{2\pi}{\hbar} \sum_k (t_{ki}^\chi)^* t_{kj}^\chi \delta(\epsilon_k^\chi - E_1 + E_0)$$

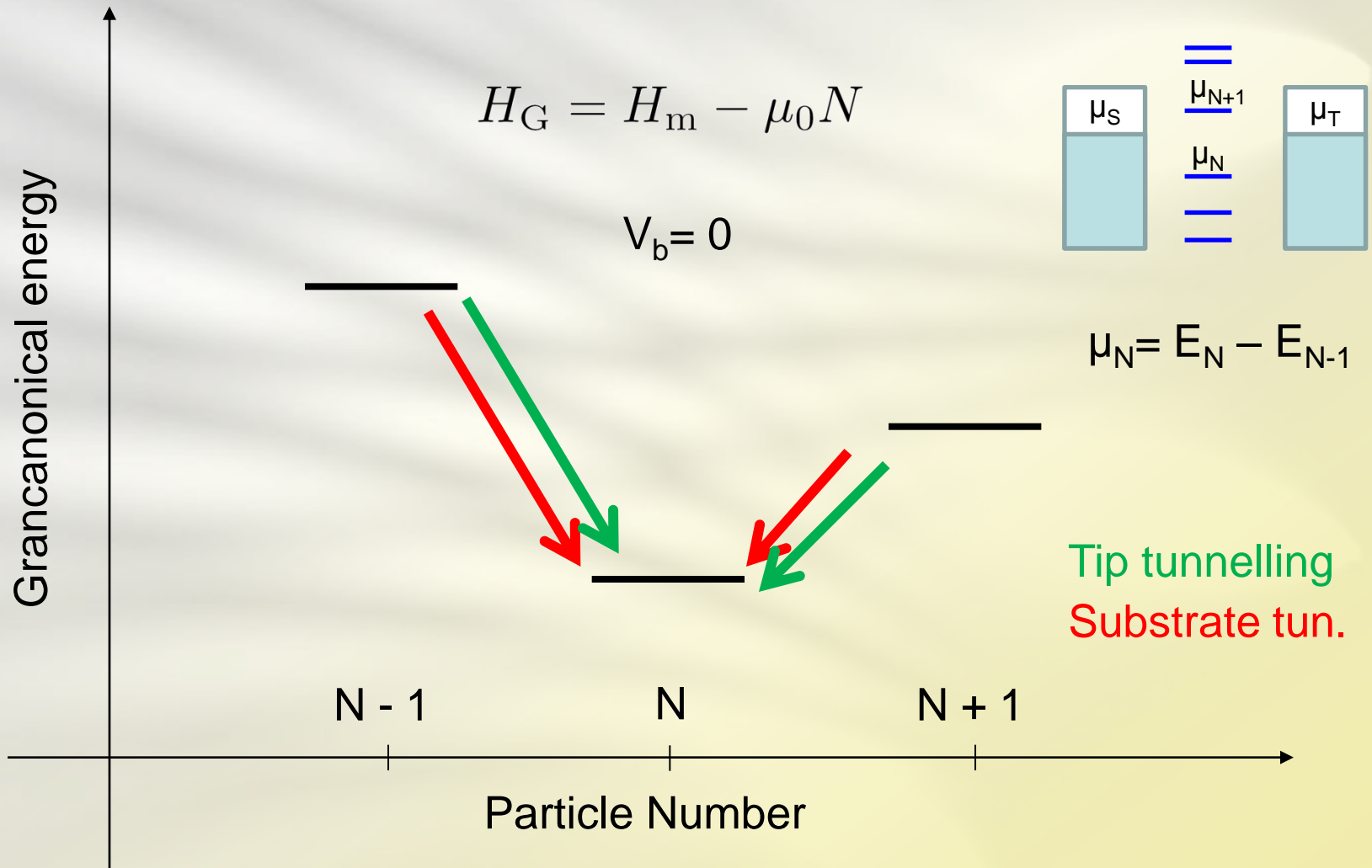
For **uncorrelated** and **non-degenerate systems** the many-body rate reduces to

$$R_{N E_0 \rightarrow N+1 E_1}^{\chi\tau} = \Gamma_{\text{orb}}^\chi(\epsilon_{\text{orb}}) f^+(\epsilon_{\text{orb}} - \mu_\chi)$$

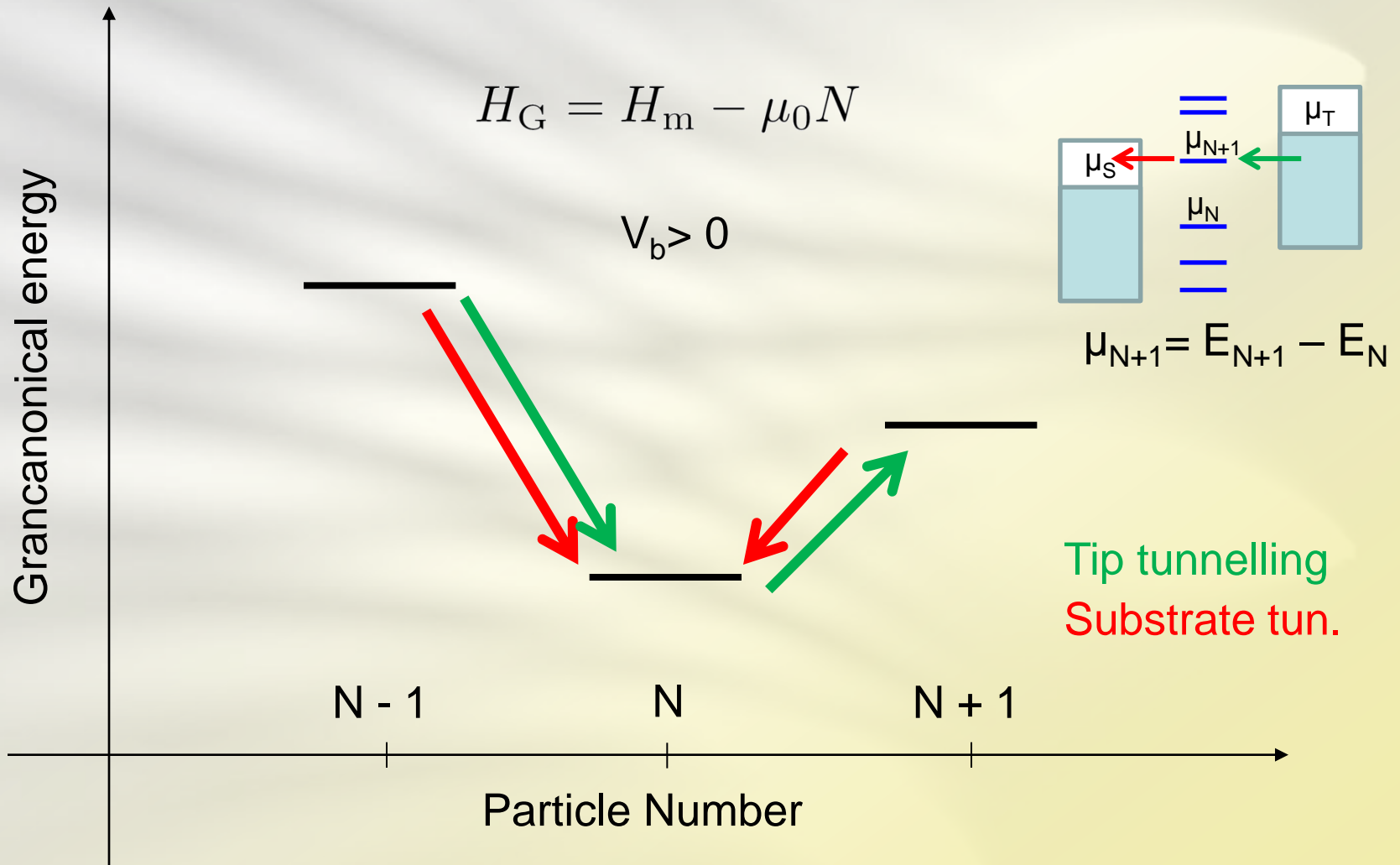


The **constant current map** is the **isosurface** of a **specific molecular orbital**.

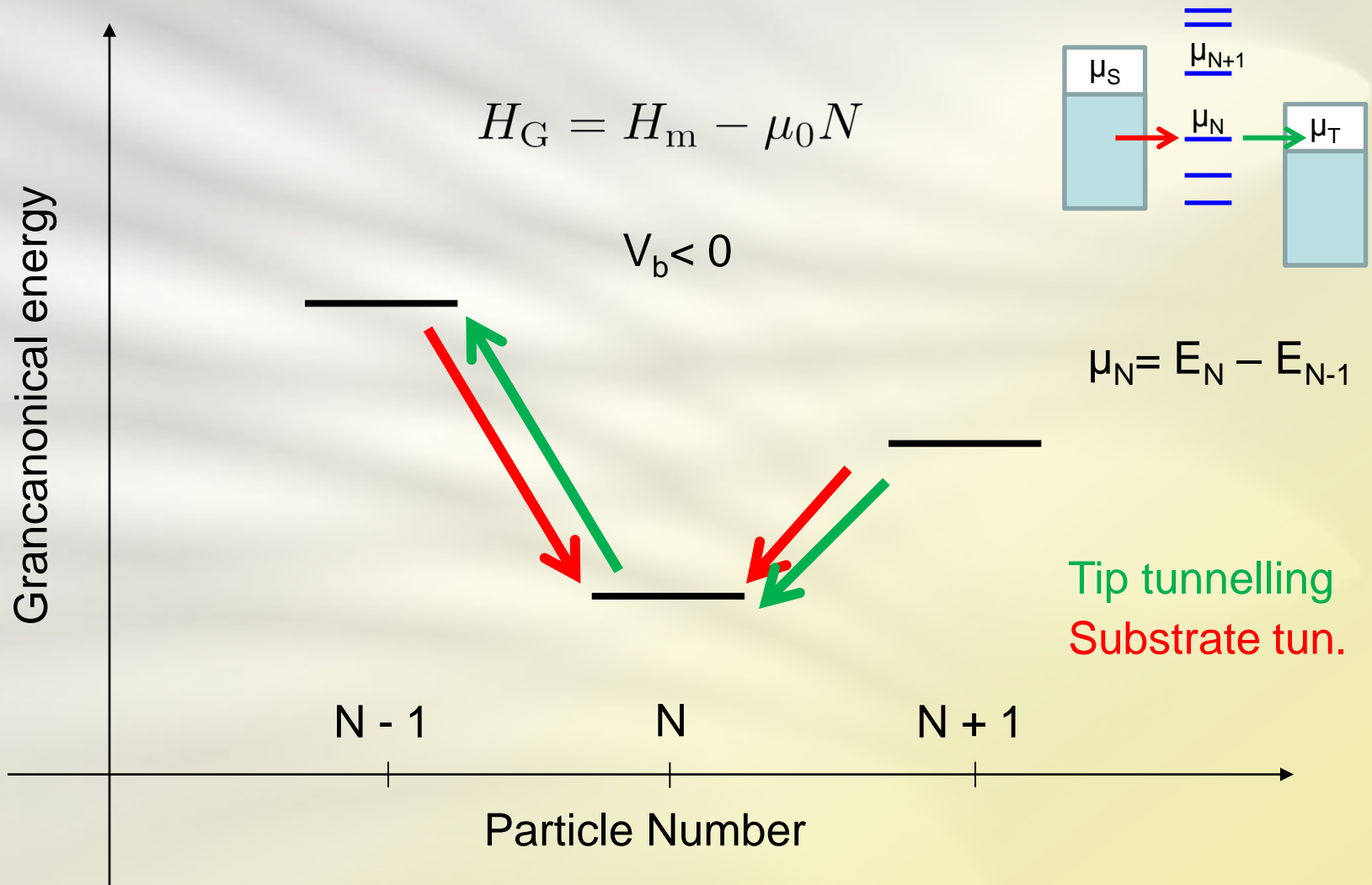
Dynamics in energy space



Dynamics in energy space

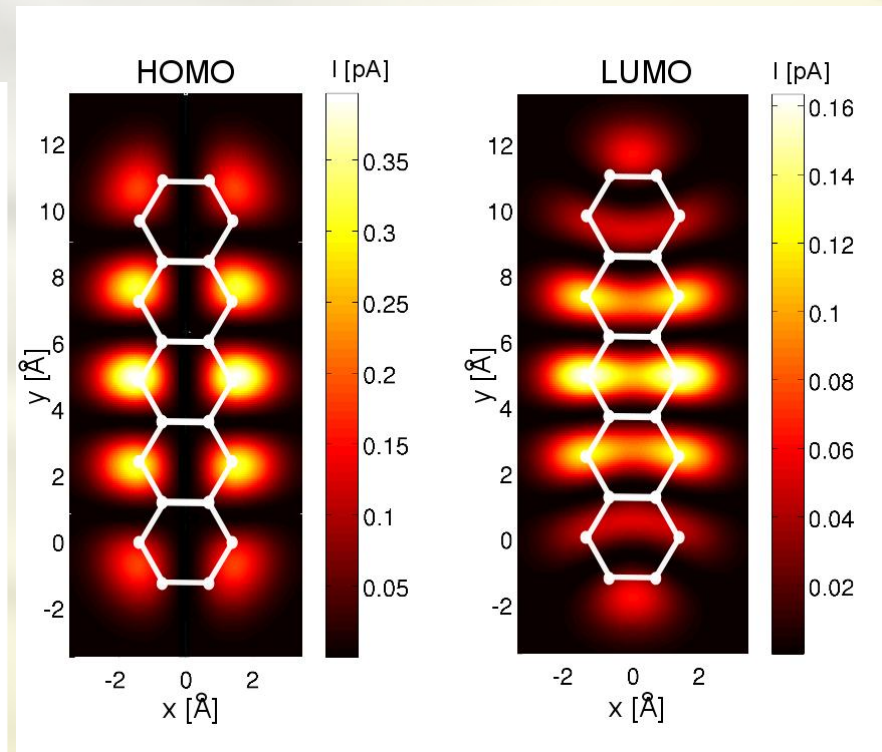
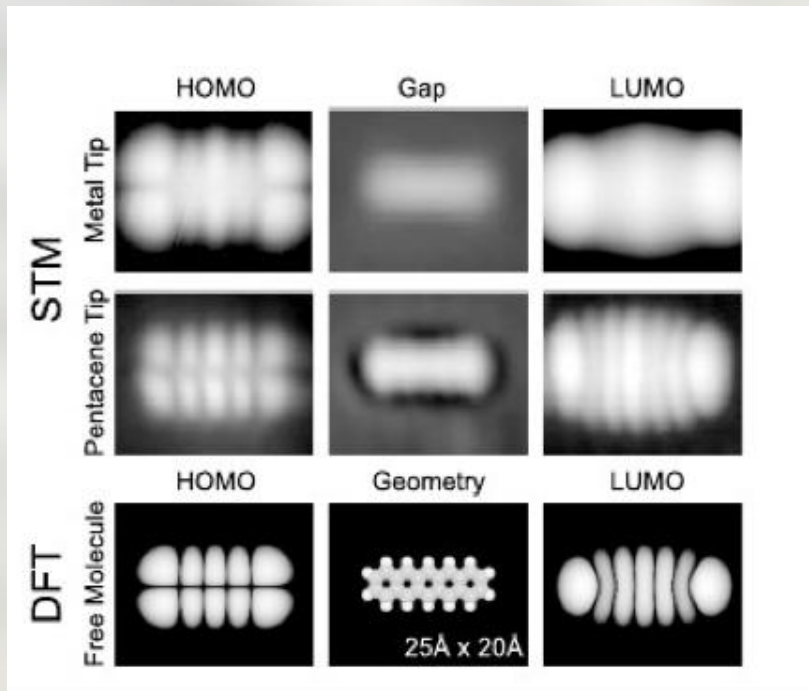


Dynamics in energy space



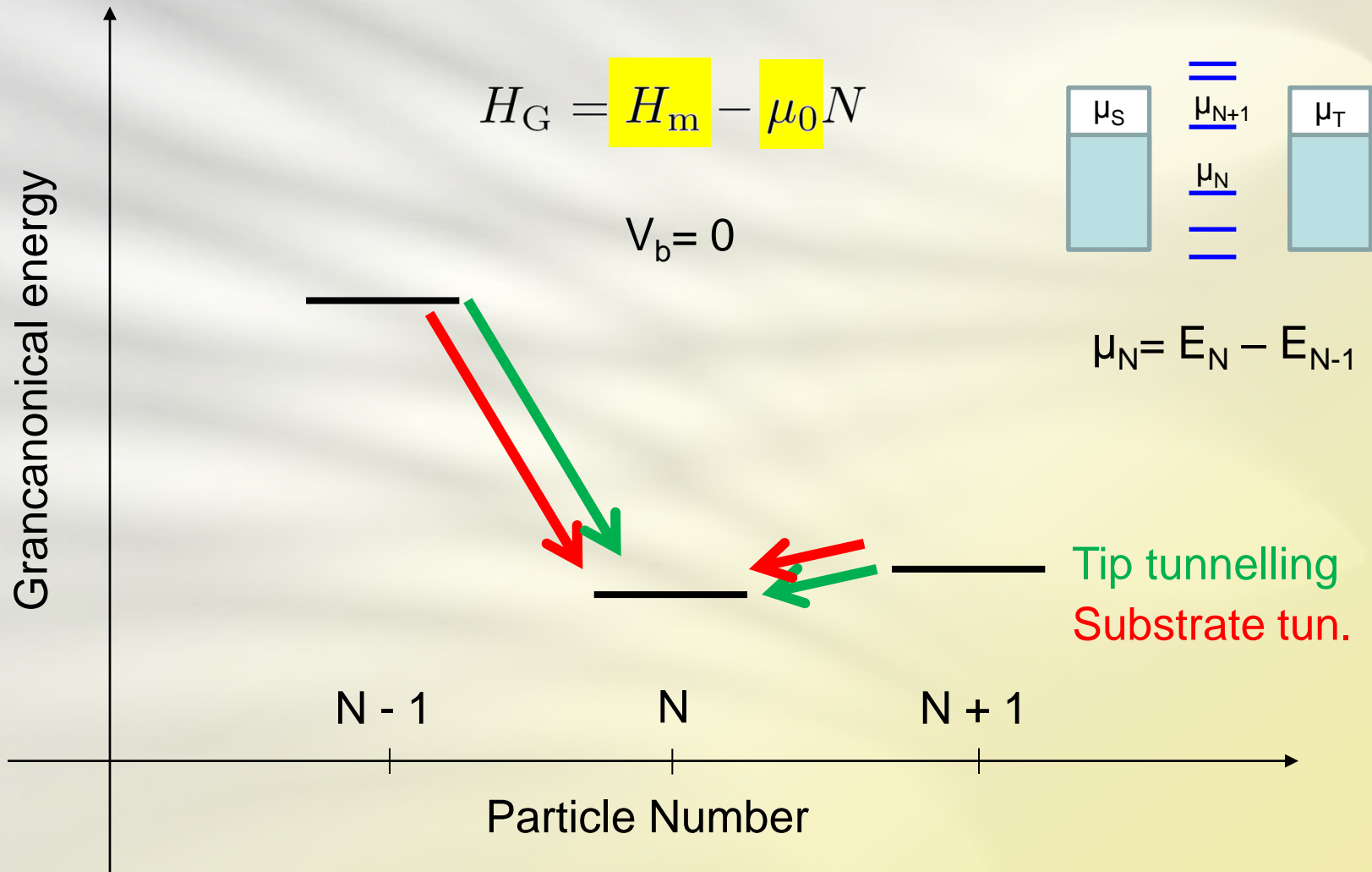
Visualization of molecular orbitals

Topography

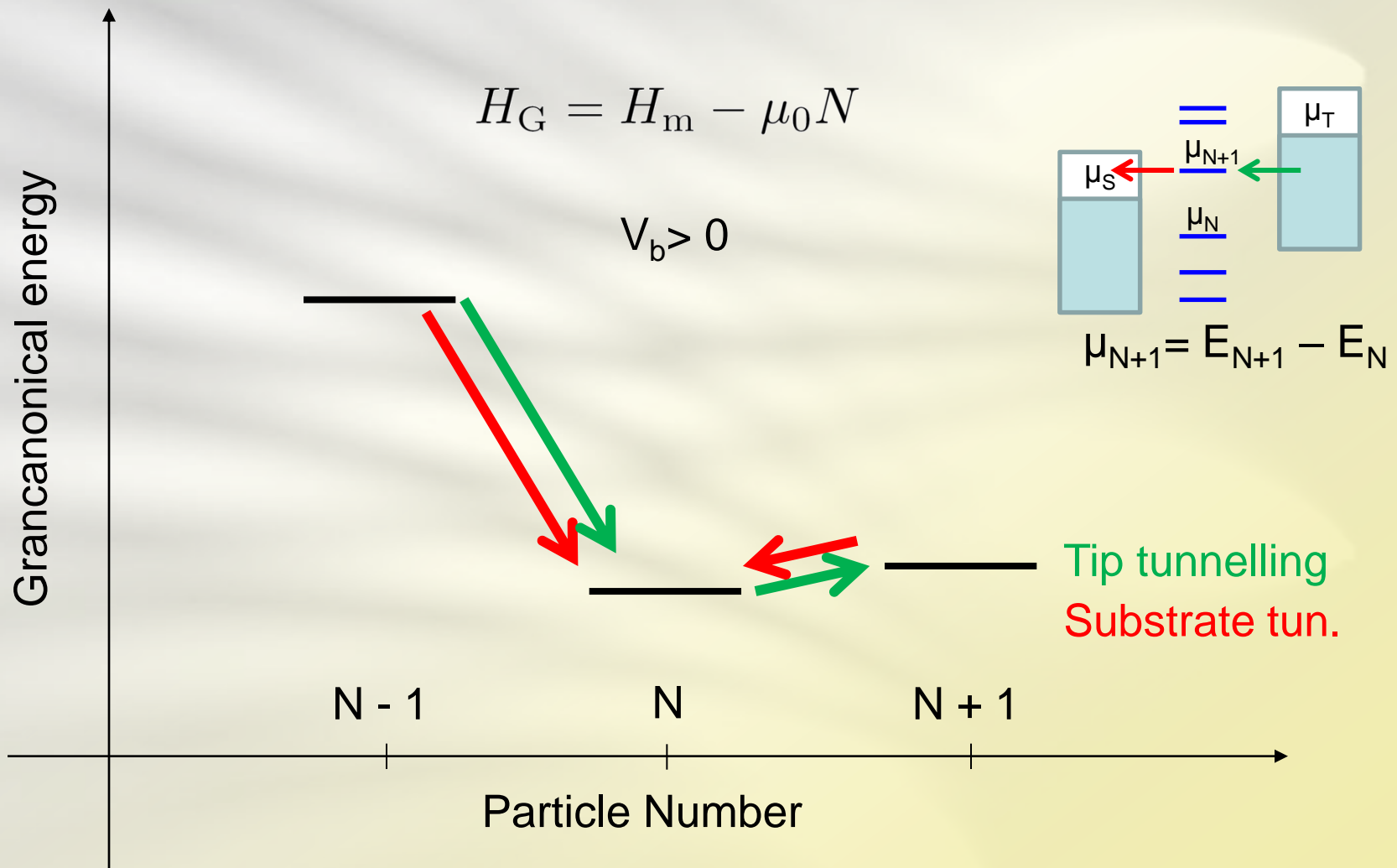


J. Repp and G. Meyer, Physical Review Letters **94**, 026803 (2005)

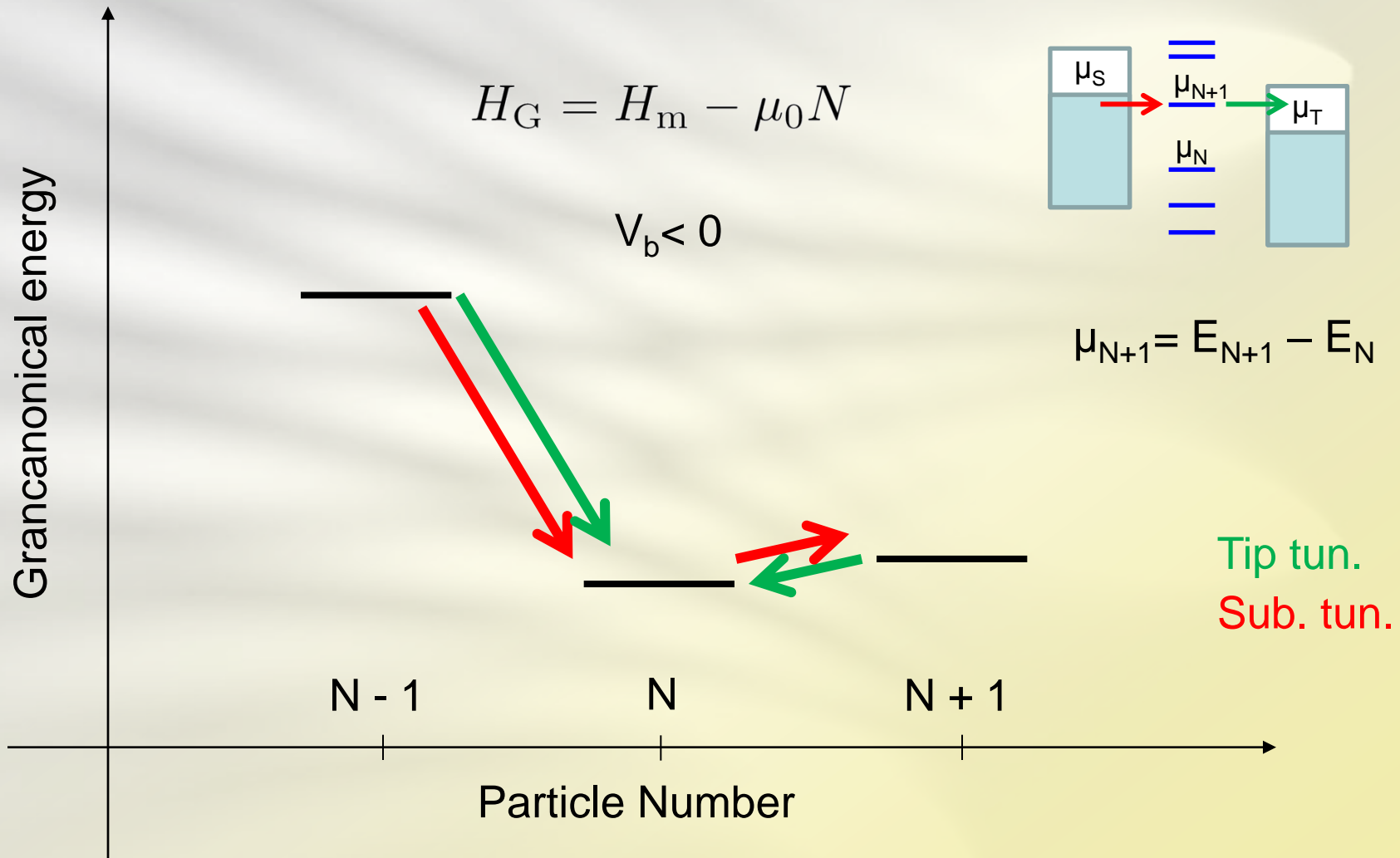
Dynamics in energy space



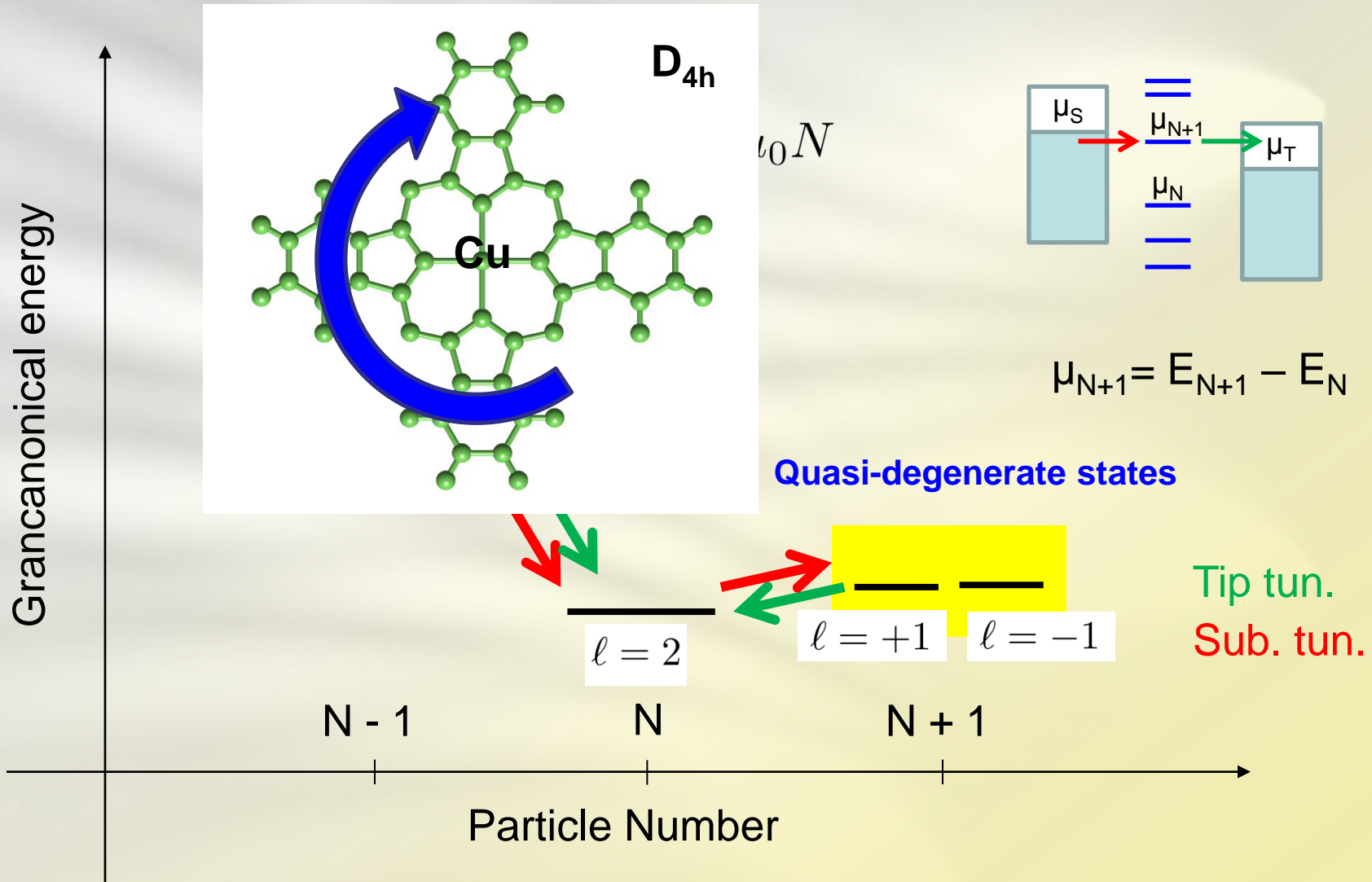
Dynamics in energy space



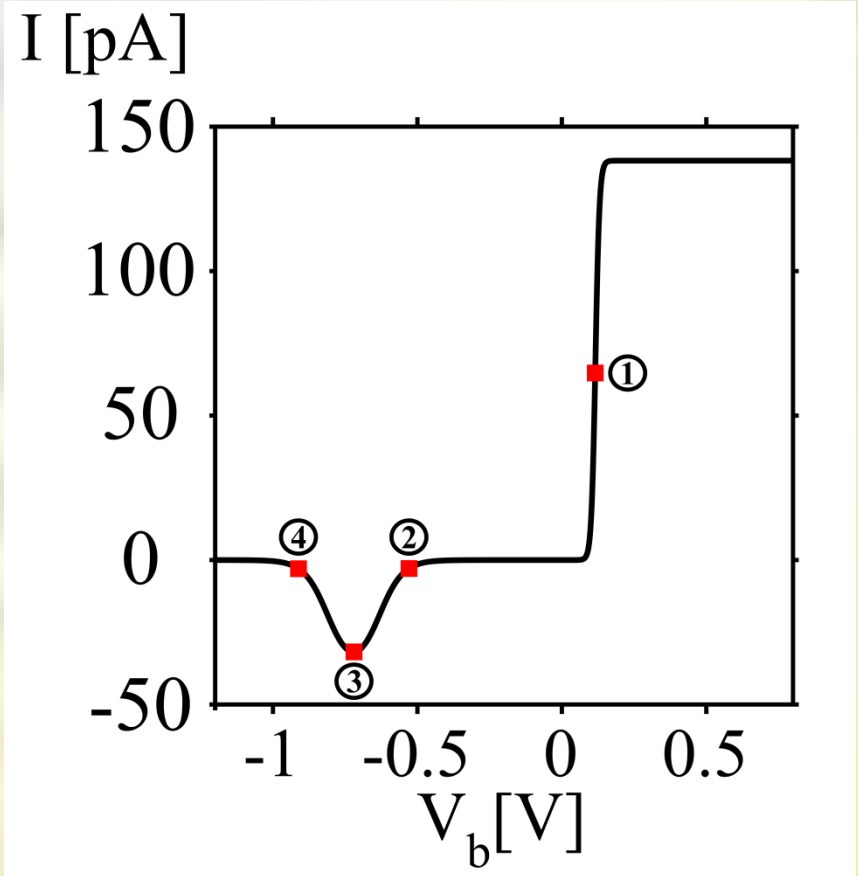
Dynamics in energy space



Dynamics in energy space

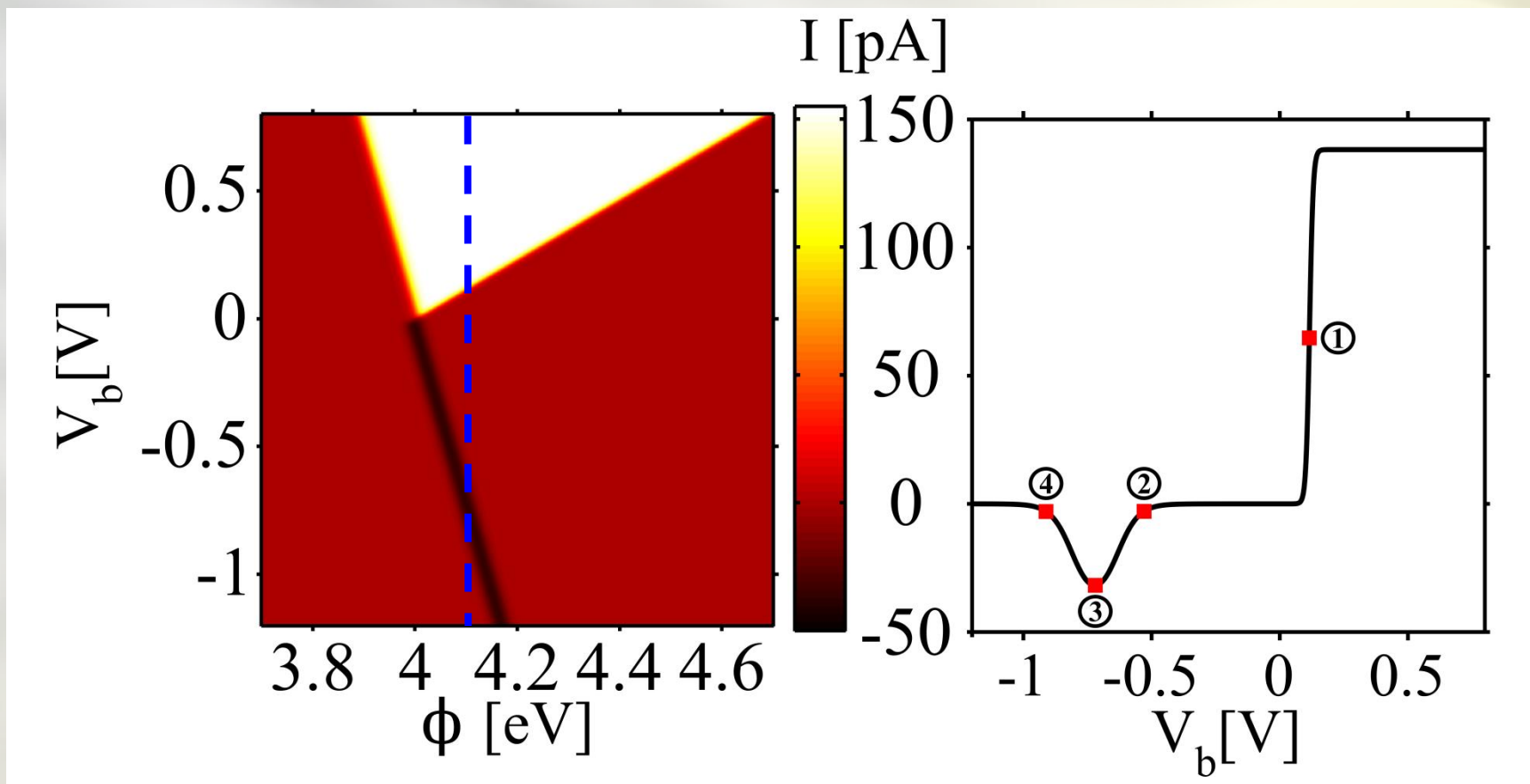


Interference blocking



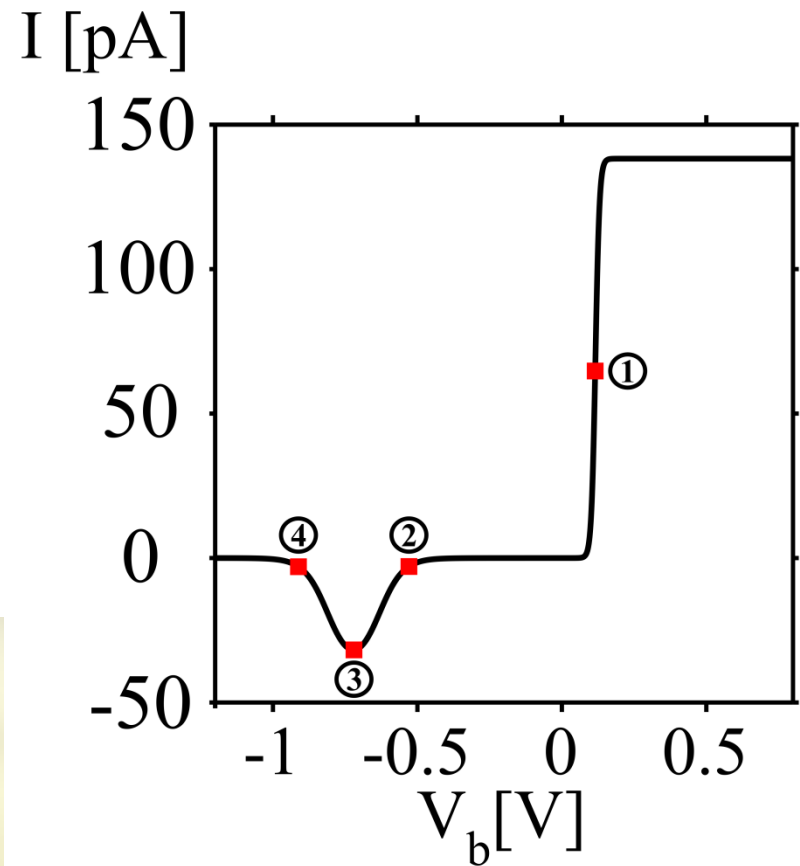
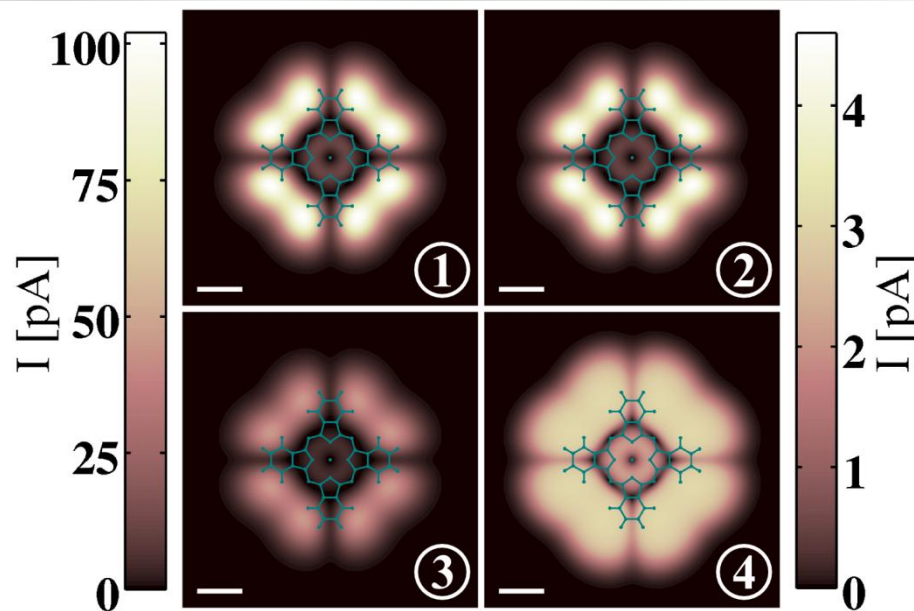
Donarini, Siegert, Sobczyk and Grifoni **Phys. Rev. B** 86, 155451 (2012)

Interference blocking



Donarini, Siegert, Sobczyk and Grifoni **Phys. Rev. B** 86, 155451 (2012)

Topographical fingerprint



(e)

Experiment:
Cu-Pc on
two-atomic-layer NaBr

W. Ho et al.
PRL 100, 126807 (2008)

B

Donarini, Siegert, Sobczyk and Grifoni
Phys. Rev. B 86, 155451 (2012)

Interference blocking

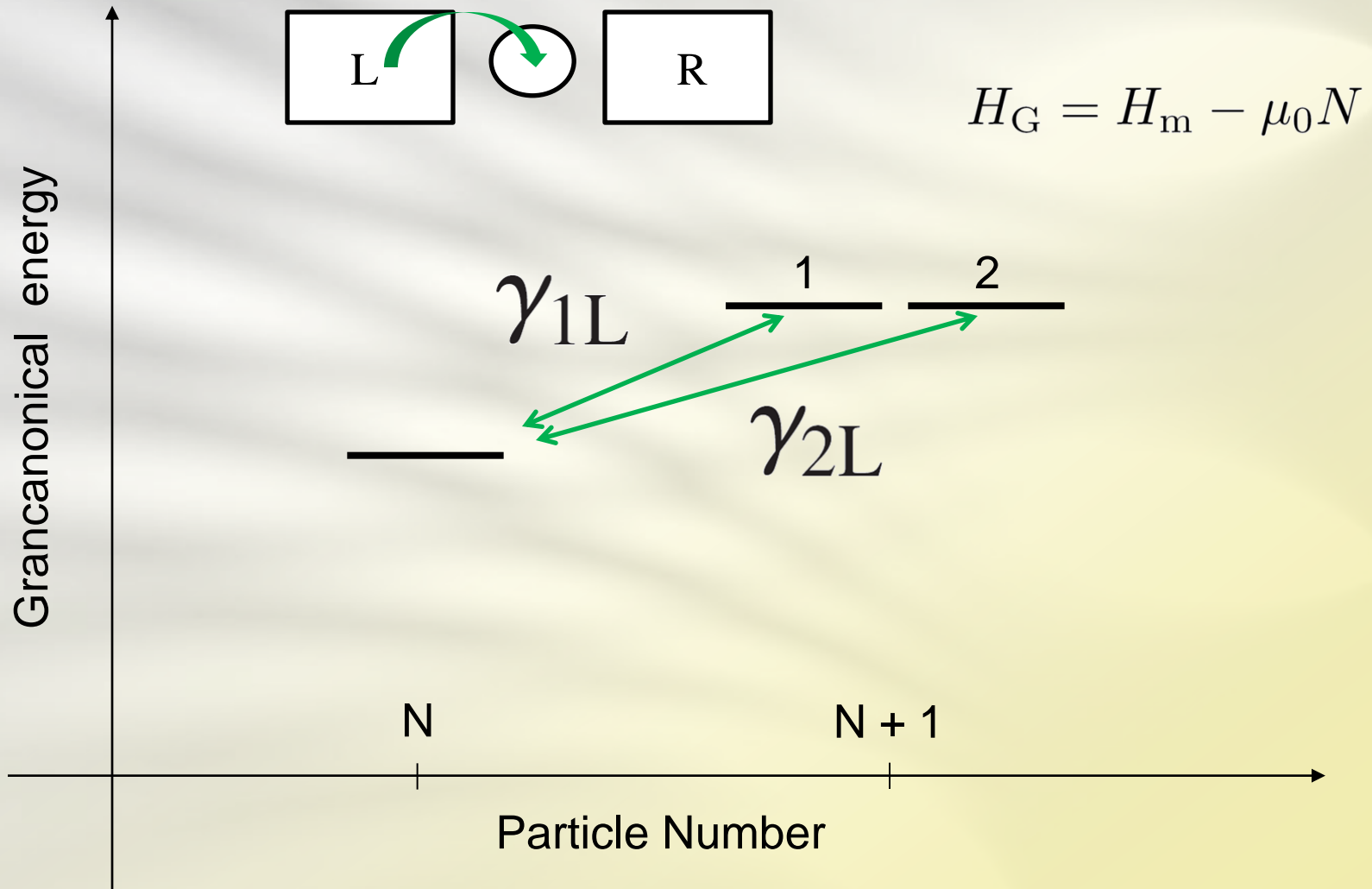
Necessary conditions:

1. **Quasi-degeneracy** of the anionic ground state (e.g. Due to rotational symmetry);
2. **Electron affinity** approximately **equals** the (effective) substrate **work function**.

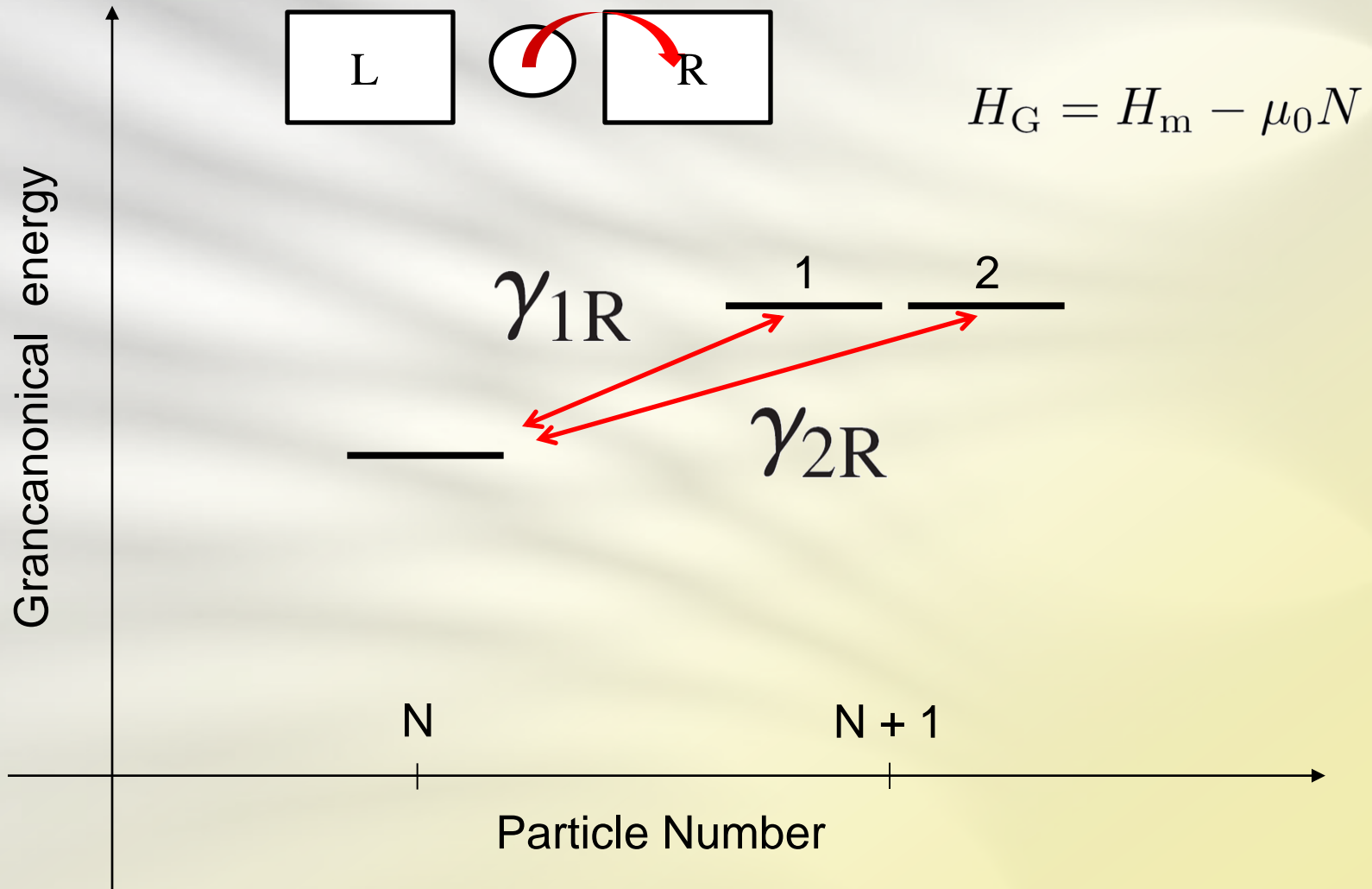
Fingerprints:

1. Strong **negative differential conductance** at **negative sample biases**;
2. **Flattening** of the **constant height current images** in the vicinity of the interference blockade regime.

Many-body tunnelling amplitudes



Many-body tunnelling amplitudes



Contact symmetry breaking

$$|1'\rangle = a|1\rangle + b|2\rangle \quad \Rightarrow \quad \gamma_{1'L} = a\gamma_{1L} + b\gamma_{2L}$$

$$\boxed{\frac{\gamma_{1L}}{\gamma_{2L}} \neq \frac{\gamma_{1R}}{\gamma_{2R}}} \quad \Rightarrow \quad \exists \begin{array}{l} |1'\rangle \\ |2'\rangle \end{array} \quad \begin{array}{l} \gamma_{1'L} \neq 0 \\ \gamma_{1'R} = 0 \\ \gamma_{2'L} \neq 0 \\ \gamma_{2'R} \neq 0 \end{array}$$

More degenerate states? See
 A. Donarini, G. Begemann, and M. Grifoni *Phys. Rev. B*, **82**, 125451 (2010)
 for the general theory.

Interference: decoupling basis

Degenerate anionic ground state



Matrix form for the **many-body tunnelling rate** between the neutral and anionic ground states.

Angular momentum basis

Decoupling basis

Tip

$$\mathbf{R}^T = R_0^T \begin{pmatrix} \overset{\ell=+1}{1} & \overset{\ell=-1}{e^{-2i\phi}} \\ e^{-2i\phi} & 1 \end{pmatrix}$$

Mixes angular momentum

$$\tilde{\mathbf{R}}^T = R_0^T \begin{pmatrix} 2 & 0 \\ 0 & 0 \end{pmatrix}$$

One of the anionic state is **decoupled from the tip**

Substrate

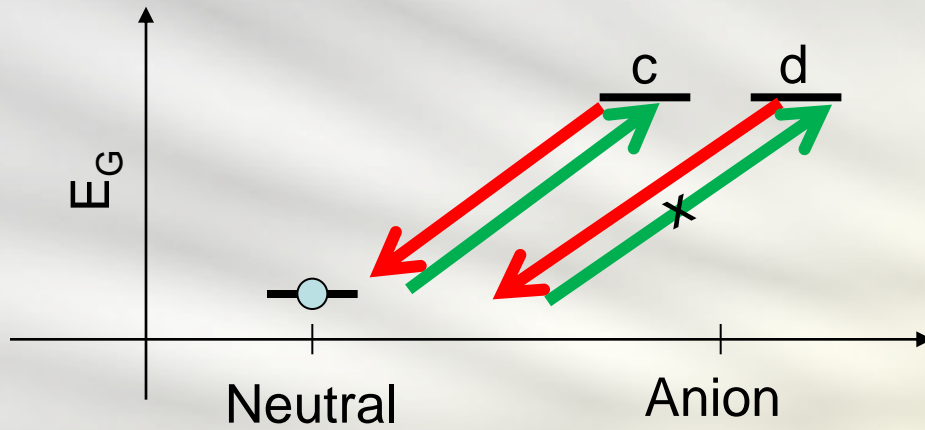
$$\mathbf{R}^S = R_0^S \begin{pmatrix} 1 & 0 \\ 0 & 1 \end{pmatrix}$$

Conserves angular momentum

$$\tilde{\mathbf{R}}^S = R_0^S \begin{pmatrix} 1 & 0 \\ 0 & 1 \end{pmatrix}$$

Notice that the decoupling basis **depends** on the **tip position**.

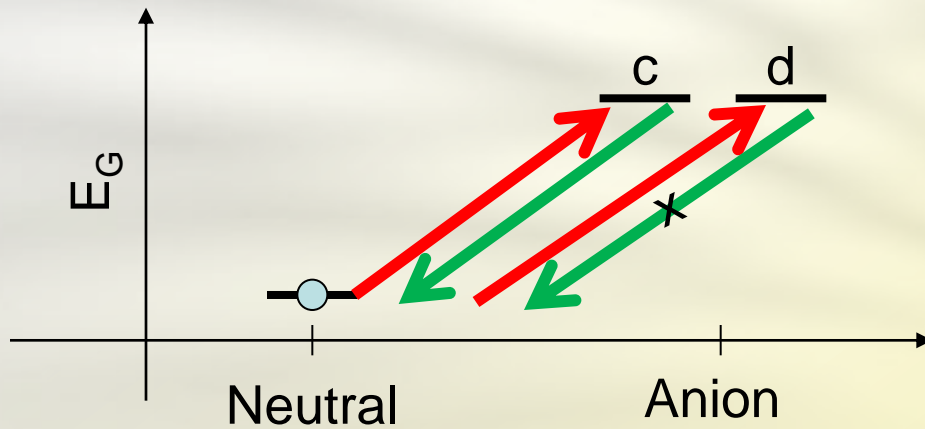
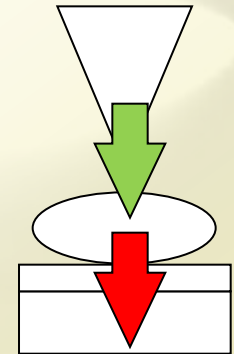
Interference: current blocking



$$V_b > -\Delta E_G / ec$$



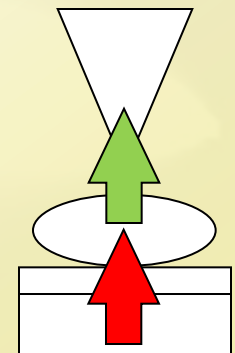
Current



$$V_b < \Delta E_G / e(1 - c)$$

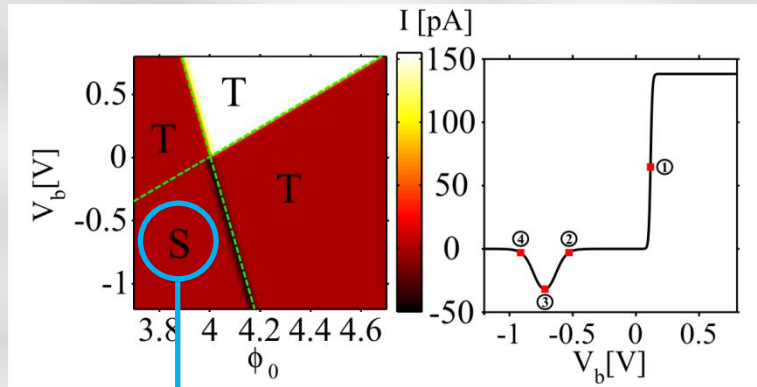


No current

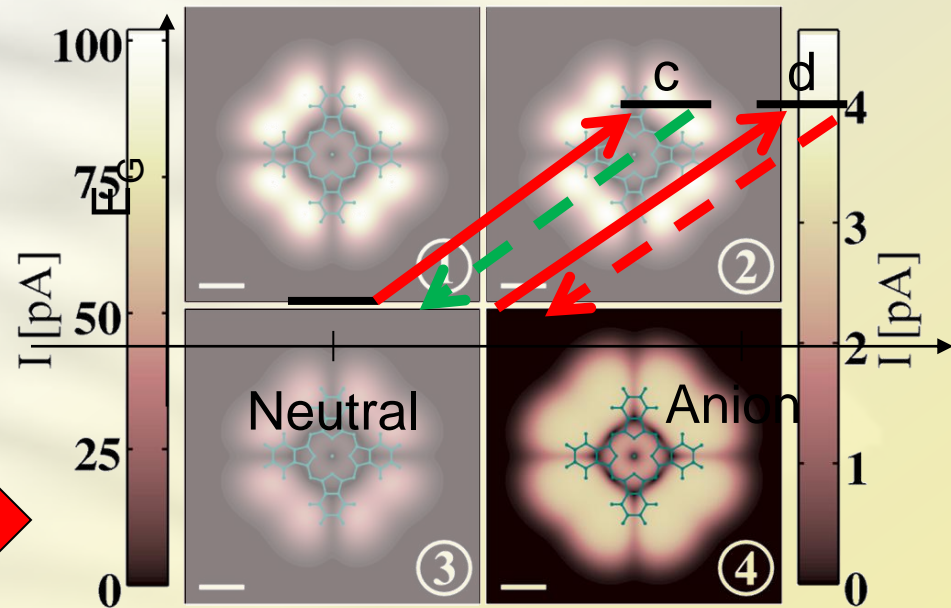
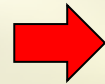


$$\mu_T = \mu_0 - ceV_b \quad \mu_S = \mu_0 + (1 - c)eV_b \quad c \approx 0.9$$

A new bottle-neck process



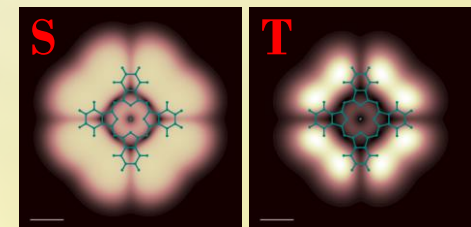
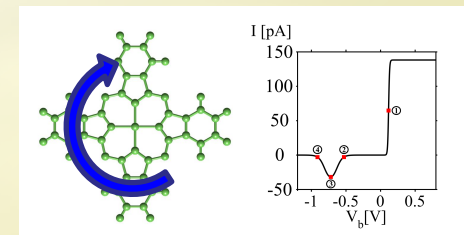
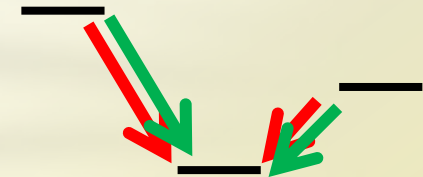
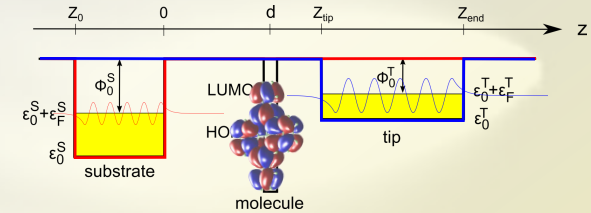
$$I_{IB} = e \frac{R_0^S f_S^- R_0^T f_T^-}{R_0^S f_S^- + R_0^T f_T^-}$$



The **depopulation** of the blocking state via a **substrate transition** dominates the transport.

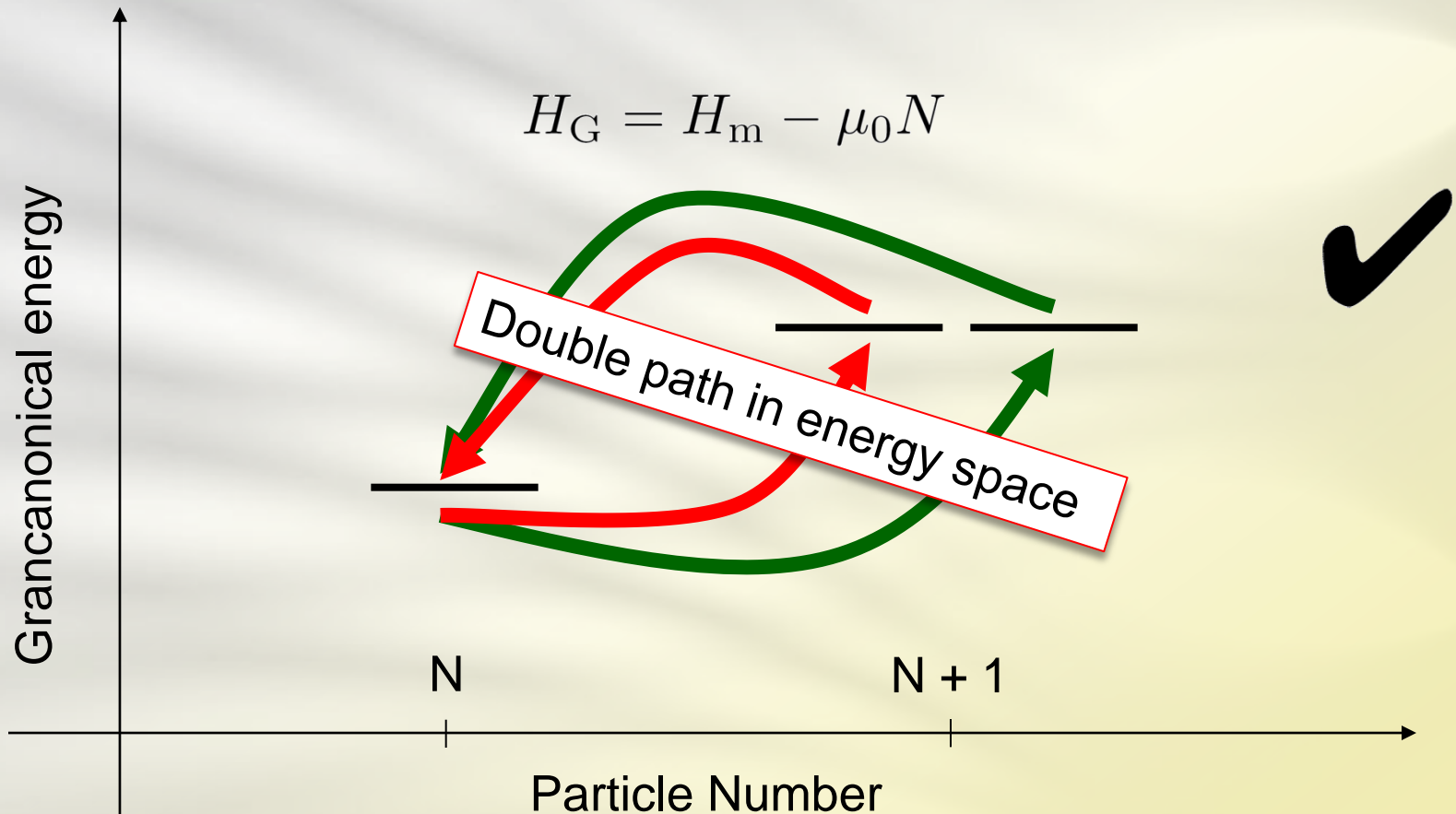
Conclusions

- We developed a **semi-quantitative model** for the description of “weakly coupled” STM junctions with π -conjugated molecules.
- The dynamics is described in terms of **many-body** transitions.
- Transport through **degenerate states** is associated to **electron interference** blockade at negative sample biases.
- Close to the interference blocking regime, substrate tunnelling dominates the transport and gives **flat constant height current maps**.



Interference Resonance

Interference + interaction



Donarini, Begemann, and Grifoni, *Phys. Rev. B* **82**, 125451 (2010)

Outlook



- Improve the description of the electron-electron interaction to include **correlation effects** (exchange, magnetic anisotropy...)
- Include **molecular vibrations** to investigate their impact on interference phenomena
- Study the effect of **spin polarized current injection**
- Include **higher order tunnelling** effects (co-tunnelling, Kondo)

Thanks



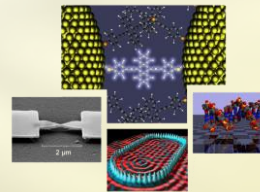
Benjamin Siegert



Sandra Sobczyk



Milena Grifoni



SPP 1243



SFB 689

Thank you for your attention...

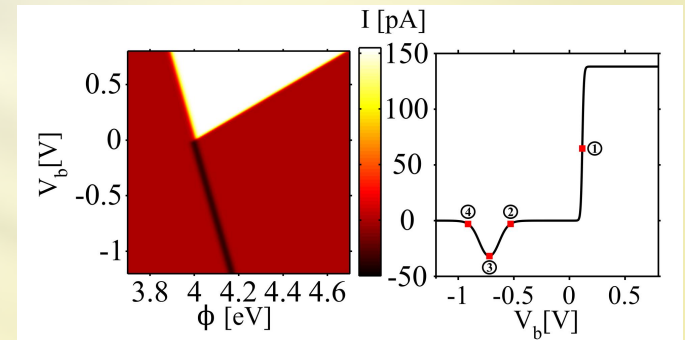
Dynamics in a reduced space

$$\begin{pmatrix} \dot{\sigma}^N \\ \dot{\sigma}_c^{N+1\tau} \\ \dot{\sigma}_d^{N+1\tau} \end{pmatrix} = \left[2R^T \begin{pmatrix} -2f_T^+ & 2f_T^- & 0 \\ f_T^+ & -f_T^- & 0 \\ 0 & 0 & 0 \end{pmatrix} + R^S \begin{pmatrix} -4f_S^+ & 2f_S^- & 2f_S^- \\ f_S^+ & -f_S^- & 0 \\ f_S^+ & 0 & -f_S^- \end{pmatrix} \right] \begin{pmatrix} \sigma^N \\ \sigma_c^{N+1\tau} \\ \sigma_d^{N+1\tau} \end{pmatrix}$$

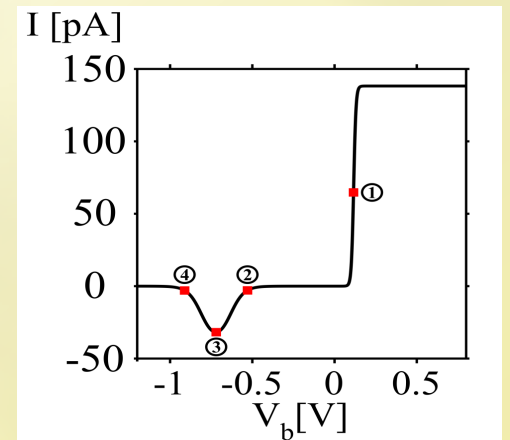
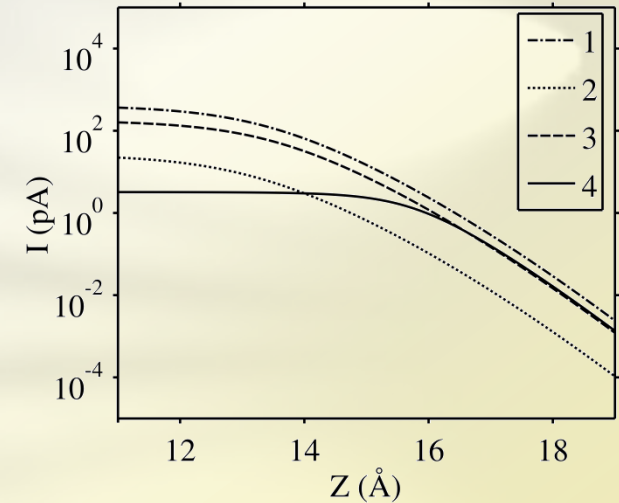
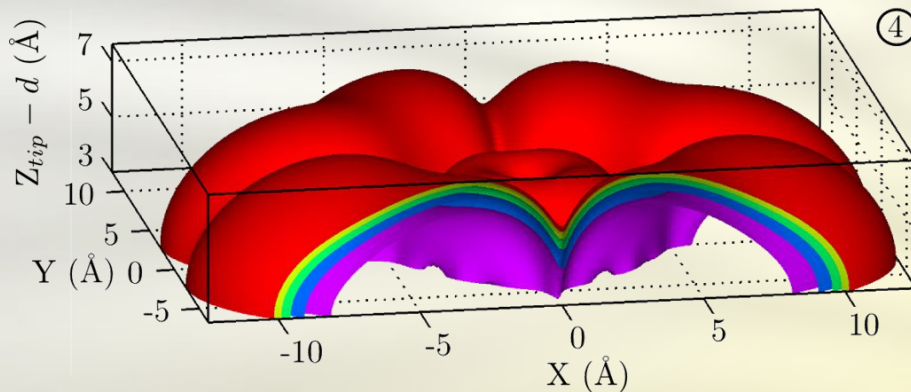
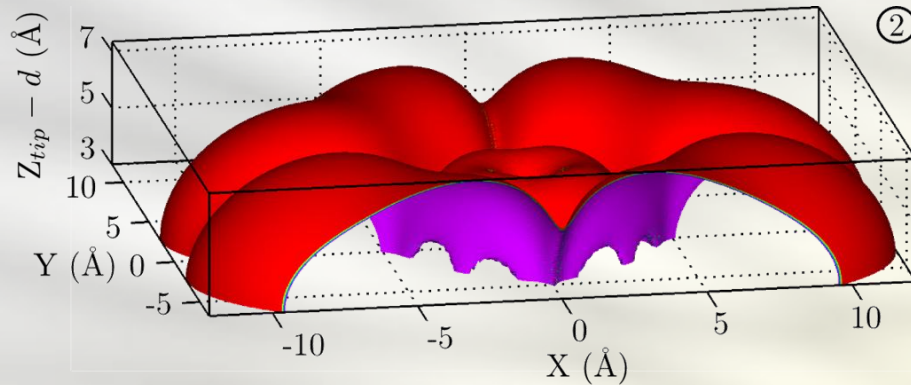
$$I(\vec{R}_{\text{tip}}, V_b) = 2eR^S f_S^+ \sigma^N \left(1 - \frac{\sigma_c^{N+1\tau}}{\sigma_d^{N+1\tau}} \right)$$

$$\sigma^N = \left(1 + 2 \frac{R^S f_S^+ + 2R^T f_T^+}{R^S f_S^- + 2R^T f_T^-} + 2 \frac{f_S^+}{f_S^-} \right)^{-1}$$

$$\frac{\sigma_c^{N+1\tau}}{\sigma_d^{N+1\tau}} = \frac{R^S f_S^+ + 2R^T f_T^+}{R^S f_S^- + 2R^T f_T^-} \cdot \frac{f_S^-}{f_S^+}$$



Constant current maps



Constant current maps calculated
at working currents: $I = 3.15, 3.075, 3.0, 2.925,$ and 2.85 pA